

Sensors & Actuators, B: Chemical

Full length research papers

Session: Chemical actuators-soft actuators

Enhancement of deformation of redox-active hydrogel as an actuator by increasing pendant viologens and adding filler or counter-charged polymer

Bo Wang^a, Hironobu Tahara^b, Takamasa Sagara^{b,*}

^a *Department of Advanced Technology and Science for Sustainable Development, Graduate School of Engineering, Nagasaki University, Nagasaki 852-8521, Japan*

^b *Division of Chemistry and Materials Science, Graduate School of Engineering, Nagasaki University, Bunkyo 1-14, Nagasaki 852-8521, Japan*

Keywords: Soft actuator; Deformation; Hydrogel; Viologen; Conductive filler; Poly-ion complex

* Corresponding author

E-mail address sagara@nagasaki-u.ac.jp

Graphical Abstract



Highlights

- PLLV-GA-gel floating in water was reduced by dithionite and re-oxidized by O₂.
- The optimal pendant amount for quick deformation was one viologen per four Lys units.
- The use of fillers, AuNP, graphene, and CNT accelerated reductive contraction.
- Partial complexation with poly-anion accelerated the swelling upon re-oxidation.

ABSTRACT

Strategies for enhancement of redox-driven deformation of a hydrogel, viologen pendant poly-*L*-Lysine based glutaraldehyde cross-linked hydrogel (PLLV-GA-gel), were pursued. To surpass the previously reported fastest reductive contraction, a 93% volume decrease within 100 s on dithionite reduction, and to accelerate expansion on oxidation, we examined the pendant rate dependence and the effect of the addition of conductive fillers or an anionic polymer, poly(styrene sulfonate) (PSS). In testing deformation of water-floated PLLV-GA-gels, the contraction of a 25% pendant rate gel was greater and faster than others. The initial rate of reductive contraction of the gels with fillers was in the order of graphene nano-platelet (GNP) > gold nanoparticle > carbon nanotube (CNT) > no-filler. The initial rates of swelling of GNP and CNT gels on oxidation were faster than the no-filler gel. PSS incorporation enhanced the swelling rate and amplitude but slowed down the contraction. All the PLLV-based samples on a Au electrode showed largely diffusion-controlled redox reactions of viologen in voltammograms and radical cation dimer rich light-absorption features in electroreflectance spectra. The guide for the choice of conductive filler and coexistence of anionic polymer described herein should be applicable to enhance the deformation of many redox-driven hydrogel actuators.

1. Introduction

Among the soft actuators, highly deformable electrochemical actuators are of particular interest because of immediate biomedical applications, light weight, power, quietness, and compactness [1,2]. To mention just two representative redox-driven polymer actuators, (1) autonomous biomedical robots have been targeted using a self-oscillation motivated polymer gel by the Belousov-Zhabotinsky reaction [3], and (2) electroconductive polymer such as poly(3,4-ergylenedioxythiophene)-based ones have been extensively investigated [3]. In addition to these, attention have recently payed to redox driven hydrogels that show reversible deformation in response to external stimuli, because quick and reversible redox reactions give fast and large-amplitude deformation of the gels and find application as actuators [4-19]. When using polymer-based hydrogel actuators, their deformation is frequently limited by the inefficient transmission of the redox diving force throughout the gel [4]; if the gels are not electronic conductors, electro-osmotic and diffusion processes act as intermediate steps for deformation. Reversibility and quickness of the deformation are the keys to realize a flexible and self-directive motility of a molecular robot that is composed of a gel actuator. To attain such redox-driven deformable hydrogels as actuators, there are mainly three ways: incorporation of electronic conductive polymers [4,5], conductive fillers [6], and reversible redox sites with a high density. Recently, the last way has extensively investigated using ferrocene [7-11], hydroquinone [12,13], and viologens [14-19]. Some of them are combined with photo-excitation induced redox reaction [16-19].

A deformable molecular robot may be directly placed on an electrode surface in water, on which direct electron transfer processes can readily drive the redox actuation of the gel. We imagine an ameba-like gel crawling on a solid electrode surface. The electrode surface plays two roles: (i) energy supply to attain fast, reversible, and repeatable locomotion with a large amplitude and (ii) fine and precise regulation of the movement. Such a gel may find applications to a directional walking soft robot that can work where conventional mechanical robots cannot, waste treatment and collection of biological or mineral resources, and a local tissue healing soft robot, with no need to say anymore to biomedicine as micro pumps, deformable smart textiles, and alternative biomimetic functional systems.

With an aim at developing redox driven hydrogel actuators, we reported a redox active viologen-based hydrogel [14]. We attached viologens covalently via an amide linkage to the

side-chain of a poly-peptide, α -poly-*L*-lysine (PLL). Then, we used glutaraldehyde (GA) to cross-link free ϵ -amine sites of PLL to obtain the hydrogel, PLLV-GA-gel (Fig. 1-a). The hydrogel with a 25% viologen pendant rate contracted by deswelling down to 7%-volume of the initial in 100 s upon reduction of viologens by dithionite [14]. One-electron reduction of a viologen dication (V^{2+}) to viologen radical cation ($V^{\bullet+}$) induces stacking of $V^{\bullet+}$ units and desolvation from the viologen sites. The stacking process to form $V^{\bullet+}$ dimers hauls the polymer chains to entangle them and accelerates inter-site electron transfer processes. Simultaneously, the desolvation process drains water from the gel. A decrease of positive charges on viologens upon reduction results in the change of osmotic pressure and helps water egress from the gel. All these changes upon reduction contribute to the contraction of the hydrogel.

Fig. 1

However, re-expansion of contracted PLLV-GA-gel by re-swelling through the re-oxidation of $V^{\bullet+}$ in O_2 saturated water was slow [14]. The gel re-expansion was limited to about half the initial size. The quickness and amplitude were far beneath our tentative goal, swelling back from 10%-relative volume to 100% in 100 s. Considering the re-expansion of the completely shrunk PLLV-GA-gel in the reduced state, some of the elemental processes should be sluggish: penetration of a reductant into the gel, electron transfer to oxidize $V^{\bullet+}$, and ingress of water into the gel. Enhancement of the deformation requires the acceleration of these elemental processes.

For strategic enhancement of the deformation, we first test PLLV-GA-gels with various viologen pendant rates, the number of the pendant viologens per total number of the lysine units, ξ . A finding of the optimal ξ for the redox deformation is of profound importance, because the concentration of the redox site and the kinetics of electron transfer are in a trade-off relation in many redox polymers [20].

A question we asked by ourselves is whether there may be a better cross-linker than GA. Rodriguez et al. demonstrated that a hydrogel of ammonium group-modified hydroxylcellulose was cross-linked by glycol diglycidyl ether (EGDE) to produce a superabsorbent in water [21]. It is also pointed out that cross-linking of amine groups by EGDE enhances mechanical stability, though its short linkage tends to suppress segmental dynamics [22]. The GA linkage provides linking length variety and flexibility on the basis of the Schiff base bonding, which is, however,

susceptible to acid hydrolysis. Therefore, using the PLLV with the best region of ξ , we compare the behavior of GA cross-linked PLLV-GA-gel (Fig. 1-a) to EGDE cross-linked PLLV (PLLV-EGDE-gel, Fig. 1-b) and GA cross-linked PLL with non-covalently penetrating precursor carboxylated viologen (PLL-GA + BCV, Fig. 1-c).

Then, we closely explore the effect of incorporation of conductive fillers, gold nanoparticle (AuNP), graphene nano-platelet (GNP), and single-walled carbon nanotube (CNT). The rationale behind our use of these fillers can be supported partly by previous relevant reports. So far, incorporation of Au nanostructures in a hydrogel has been tested to enhance photo response. For example, Guo et al. fabricated Au-nanostructure-poly(*N*-isopropyl acrylamide) hydrogel with control over the spatial distribution of Au [23]. They irradiated a laser light beam to locate photo-thermal heating to sharply deform the thermo-responsive hydrogel. Ohnishi et al. synthesized dendritic fractal Au deposits in a perfluorocarboxylic acid membrane solid polymer electrolyte actuation gel to achieve non-faradaic electrochemical deformation [24,25]. Their Au deposits were continuous bodies connected as a thin electrode, which deforms together with the gel. In our case, PLLV-GA-gel should not be anchored always to the electrode surface, because the gel should crawl on the surface. Park et al. reported that shrinkage of bacterial cellulose hydrogels containing AuNP (20 nm diameter) by its drying process to sharply increase the density of hot spots that exhibit Au-nanogap-based plasmon excited surface-enhanced Raman scattering [26]. The interparticle distance at the hot spot may enable electron conduction between the particles. Therefore, it is expected that AuNPs in PLLV-GA-gel will be closer in distance during the process of reductive contraction and act to form an electron conduction pathway, which further accelerates the reduction of viologen even far away from the electrode surface. Cai et al. synthesized a poly(vinyl alcohol) based composite hydrogel with Ag nanoparticles and enzymic hydrolysis lignin [27]. The hydrogel exhibited conductivity of 1.0 S/m. Overall, the incorporation of AuNP is a promising mean to accelerate electron transfer processes in the gel.

A number of examples to synthesize electronically conductive gels using carbon nanomaterial fillers have been reported. Recently, Guan et al. incorporated ca. 4wt% of multi-walled CNT (MWCNT) and successively attained electric conduction in the triboelectric nanogenerator and demonstrated that the conduction was restored even after the self-healing process to connect two pieces to one [28]. Lee et al. fabricated an ultra-thin 2D film of CNT

and incorporated it in an elastomer-CNT + AuNP hybrid film/hydrogel structure to achieve shape deformation upon light exposure [29].

Development of electronically conductive hydrogels for their uses in higher performance flexible devices is rapidly in progress. To mention just a few recent examples using nano-carbon fillers, Hsiao et al. prepared a paintable gelatin hydrogel precursor with MWCNT conductive fillers and a GA cross-linker [30]. The obtained gel showed an electrical resistance responsive to the mechanical deformation of the gel. Wang et al. largely enhanced electrical conduction of a poly(vinyl alcohol)-based poly(aniline)-combined hydrogel by incorporating CNT to reach conductivity of 15.3 S m^{-1} [31]. Effective uses of CNT as a conductive filler in hydrogels are also reported to achieve a conductive percolation network structure [6], to gain both electrically and mechanically higher performance [32], and to construct 3D porous flexible electrochemical sensors [33]. To synthesize flexible wearable conductive hydrogel materials, a reduced [34] and unreduced graphene oxide [35] were also used.

In the literature, however, the fabrication of hydrogel with incorporated AuNP or CNT for the acceleration of electron transfer to boost redox deformation has not been reported to the best of our knowledge. The conductive fillers are expected to form electron transfer pathways especially when the shrinkage of the gel shortens the mutual distance between the fillers.

We also conceive a strategy to enhance the deformation, incorporation of an anionic polymer, poly(styrene sulfonate) (PSS) in the PLLV-GA-gel. It has been well known that a composite film consisting poly(3,4-ethylenedioxythiophene) and PSS forms a strongly bound polymer matrix, and cation transfer between the film and aqueous [36] or non-aqueous solution [37] extensively dominates over anion transfer. The host cationic polymer can be polyaniline [38], polypyrrole [39], and poly(N-methylpyrrole) [40], and also the polyanion can be metal complexing polymeric ligands containing a number of sulfonate groups [41]. A double-layer structure of an electrode/polyaniline (ClO_4^-)/polyaniline (PSS)/solution system appeared completely as a cation selective sorption film [42].

We expect that PSS strongly binds to PLLV electrostatically at its cationic sites, namely protonated ϵ -amino groups and viologen pendants, in the hydrogel to form a poly-ion complex. It may turn out that ingress and egress processes of the counter cation of PSS occur accompanied by water drain/uptake due to the osmotic pressure difference originated by the redox of viologens in the PLLV-GA-gel. Incorporation of a counter-charged polymer may also

increase stiffness to the gel by poly-ion complexation. Too strong direct binding between the two polymers may be against the fast expansion, but a high salt concentration in the oxidized state may allow a further swelling of our PLLV-GA-gel in light of the experimental results by Zhang et al. in a viscous oily liquid state with a similar ion-complex polymer composite [43]. Therefore, we examine whether above listed effect emerges in the PLLV-GA-gel by incorporating PSS of as much as ca. 10% amount of sulfonate groups among the viologen sites in number.

Taken together, the main aim of this study includes:

- (1) Confirmation of the superiority in use of GA as the cross-linker and specification of the best pendant rate of viologen to PLL,
- (2) Exploration of the effect of conductive filler incorporation as case studies with Au-NP and nano-carbons,
- (3) Examination of the partial formation of poly-ion complex using PSS.

Present studies along with these aims should enable us to track down simple methods to enhance the deformability of the PLLV hydrogels driven by redox reaction of pendant side-chain viologen sites.

The characterization methods of our choice in this work include a deformation test of a gel sample floating in water and voltammetric and spectroelectrochemical measurements of the gels on a Au electrode surface, keeping in mind that our ultimate target is the fabrication of a molecular robot crawling on an electrode surface.

2. Materials and methods

2. 1. Materials

1-Benzyl-1'-(7-carboxyheptyl)-4,4'-bipyridinium dibromide (BCV) was synthesized as in our previous study [14]. Poly(α -L-lysine) HBr salt (α -PLL) of Mw = 12000 (the average number of unit/chain of 94) was purchased from Peptide Institute, Inc. Osaka, Japan. Reagents used in this work include a 25 % aqueous solution of GA from Nacalai tesque, 3-(dimethylaminopropyl)-3-ethylcarbodiimide hydrochloride (EDC) from TCI, *N*-hydroxy-3-sulfosuccinimide sodium salt (sulfo-NHS) from Aldrich, EGDE from TCI, poly(sodium 4-

styrene sulfonate (PSS, average $M_w \sim 70,000$, 30 wt. % in H_2O) from Aldrich, 2-morpholinoethane sulfonic acid monohydrate (MES) from Wako, GNP (6-8 nm thickness and 25 μm wideness) from TCI, CNT (50-70% carbon basis; 1.2-1.5 nm \times 2-5 μm) from Aldrich, tetrachloroauric acid ($HAuCl_4$) from Wako, sodium borohydride ($NaBH_4$) from Nacalai tesque, and sodium dithionite ($Na_2S_2O_4$) from Kishida Chemical. All the chemicals were of reagent grade and were used without further purification. Water was purified through a Milli-Q integral (Millipore) to a resistivity $> 18 M\Omega cm$.

2.2. Synthesis of viologen-pendant PLL (PLLV)

BCV (206.37 mg, 1.5 mmol), EDC (71.88 mg, 1.5 mmol), and sulfo-NHS (40.7 mg, 0.75 mmol) were dissolved in 4.0 mL of 0.10 M MES aqueous solution of pH 5.0. The solution was stirred for 1 h while cooled in an ice bath. To the resulting solution, added was PLL (52.27 mg, 1.0 mmol of Lys-unit). Stirring at room temperature (r.t.) for 48 h produced viologen-pendant PLL polymer solution. It was subjected to ultrafiltration with a Vivaspin 500 (cutoff molecular weight of 5000, from Sartorius) by water to remove the substances other than the polymer until the filtrate does not turn blue by reduction upon addition of dithionite. Lyophilization of the solution left a yellow powder. Viologen pendant rate ξ , the rate of amidated ϵ -amino groups among the initially present total ϵ -amino groups is described as

$$\xi = \frac{[PLL-C(=O)NH-V^{2+}]}{[PLL-NH_3^+] + [PLL-C(=O)NH-V^{2+}]} \quad [1]$$

ξ could be changed by pH of the MES solution, which was adjusted by addition of 0.10 M KOH solution: $\xi = 5\%$ at pH 5.0, 25% at 6.0, 40% at 7.0, and 50% at 8.0. ξ were evaluated by 1H NMR and elemental analysis in the same way as detailed in previous report [14]. Note that ξ value has an uncertainty of $\pm 5\%$.

2.3. Synthesis of GA-crosslinked hydrogel (PLLV-GA-gel)

In 100 μL of 0.050 M phosphate salt solution (pH = 11.04, prepared from K_2HPO_4 and KOH),

PLLV (6.0 mg) was dissolved, and the solution was stirred at r.t. for 30 min. Then, the solution was left unstirred at r.t. for 24 h. Then, addition of 30 μL GA solution was followed by heating at 40°C for 24 h without stirring. The obtained hydrogel was washed with water and stored in water in a refrigerator (4°C). Note that we could obtain PLLV of $\xi = 75\%$, but its gelation with GA was unsuccessful. Therefore, the pendant rate dependence test was restricted to $\xi \leq 50\%$.

2.4. Synthesis of EGDE-crosslinked hydrogel (PLLV-EGDE-gel)

In 100 μL of 0.050 M phosphate salt solution (pH = 12.02, prepared from K_2HPO_4 and KOH), PLLV ($\xi = 25\%$, 5.4 mg) was dissolved, and the solution was stirred at r.t. for 30 min. The solution left unstirred at r.t. for 24 h. Then, addition of 10 μL EGDE was followed by heating at 40°C for 24 h without stirring. The obtained hydrogel was washed with water and stored in water in a refrigerator (4°C).

2.5. PLL gel permeated with BCV solution

PLL (25 mg, 0.435 mmol), BCV (66 mg, 0.12 mmol), and 100 μL of GA solution (as received) were dissolved in 1.5 mL of 50 mM phosphate buffer (pH = 7.0) solution (PB solution), which was then stirred at r.t. for 30 min. The solution was left unstirred at r.t. for 24 h. Then, the solution was kept at 40°C for 48 h without stirring. The obtained hydrogel was washed with water and stored in a 200 μM BCV solution in a refrigerator (4°C).

2.6. Preparation of conductive filler-incorporated PLLV-GA-gel

Citrate-stabilized AuNP to be incorporated in PLLV-GA-gel was prepared by reduction of HAuCl_4 (0.018 mmol) with NaBH_4 (0.031 mmol) in the presence of trisodium citrate (0.067 mmol). The AuNP had an average spectroscopic diameter of 6.0 nm. In 100 μL of 0.050 M phosphate salt solution (pH = 11.04, prepared from K_2HPO_4 and KOH), PLLV (6.0 mg) and 10 μL of the AuNP solution (0.013 M on a Au atomic basis) were dissolved and stirred at r.t. for 30 min. The solution left unstirred at r.t. for 24 h. Then, addition of 30 μL GA solution was followed by heating at 40°C for 24 h without stirring. The obtained hydrogel was washed with

water and stored in water in a refrigerator (4°C).

To prepare GNP-incorporated PLLV-GA-gel, in 1.0 mL of 0.050 M phosphate salt solution (pH = 11.04), GNP (1.0 mg) was dispersed by ultrasonication for 2 h. In 200 μ L suspension, 12.0 mg of PLLV ($\xi = 35\%$) was dissolved and ultrasonicated for 40 min. Then, addition of 100 μ L GA solution was followed by heating at 40°C for 24 h without stirring. The obtained hydrogel was washed with water and stored in water in a refrigerator (4°C).

To prepare CNT-incorporated PLLV-GA-gel, in 1.0 mL of 0.050 M phosphate salt solution (pH 11.04), CNT (1.0 mg) was dispersed by ultrasonication for 2 h. In 10 μ L suspension, 90 μ L of 0.050 M phosphate salt solution (pH 11.04) and 13.2 mg of PLLV ($\xi = 40\%$) were added and ultrasonication for 40 min. Then, addition of 50 μ L GA solution was followed by heating at 40°C for 24 h without stirring. The obtained hydrogel was washed with water and stored in water in a refrigerator (4°C).

2.7. Incorporation of the PSS in PLLV-GA-gel

PSS solution (1.0 μ L) was added in 200 μ L of 0.050 M phosphate salt solution (pH = 11.13, prepared from K_2HPO_4 and KOH). PLLV ($\xi = 25\%$, 11.4 mg) was dissolved in 200 μ L of 0.05 M phosphate salt solution (pH = 11.13). In the PLLV solution, 105 μ L of the PSS solution was added dropwise and stirred at r.t. for 20 min. The polymer solution was left unstirred at r.t. for 24 h. Then, addition of 50 μ L GA solution was followed by heating at 50°C for 24 h without stirring. The obtained hydrogel was washed with water and stored in water in a refrigerator (4°C). The PSS content φ is defined as

$$\varphi = \frac{[\text{PSS-SO}_3^-]}{[\text{PLL-C(=O)NH-V}^{2+}]} \quad [2]$$

and it was 11%. The use of a smaller amount the PSS solution enabled us to prepare the gel with a lower φ . Higher values of φ than 11% were not attained because of significant precipitation upon the addition of more PSS.

2.8. Deformation Test of Hydrogel

The deformation of the hydrogel upon reduction of viologen was evaluated at $23 \pm 2^\circ\text{C}$ for the floating state of some pieces of the gel (ca. 2 mm or smaller) in PB solution by adding sodium dithionite solution (ca. 2 M) as the reductant. The molar amount of dithionite was approximately 10^4 -fold excess of the amount of viologen. When the saturated contraction was reached, the gel sample surface was washed with the PB solution taking 30 s, during which no further deformation occurred. The gel was placed back in a fresh buffer solution, to which O_2 gas saturated water as the oxidant was added. Assuming the occurrence of 4-electron reduction of O_2 , the amount of O_2 was at least 5 times more equivalence of viologen. The full process was recorded by a video camera to follow the change of the shape and color of the piece, whereas the time period between contraction saturation and addition of O_2 was cut out of the data presentation. The normalized width of the gel, $w_n(t)$, with respect to the fully swelled initial state was calculated as $w_n(t) = w_t/w_0$, where w_t was the width at time t and w_0 was the initial width. Under homogeneous deformation, the volume relative to the initial state, $V(t)$, can be calculated as $V(t) = 100\% w_n(t)^3$.

Note that all the measurements described in the sections 2.8 through 2.10 were made for at least two different pieces of the samples, and the reproducibility was confirmed.

2.9. Electrochemical Measurements

A polycrystalline gold (Au) disk electrode with a geometric surface area of 0.020 cm^2 (from EC Frontier Co.) was polished with a $0.3 \mu\text{m}$ and then a $0.05 \mu\text{m}$ alumina slurry to a mirror finish and then rinsed in water. An Ag/AgCl electrode in saturated KCl solution was used as the reference electrode. A coiled Au wire served as the counter electrode. All the measurements were carried out in an argon gas atmosphere at $23 \pm 2^\circ\text{C}$ using a potentiostat (Huso, HECS 315B) in PB solution. A piece of the gel was sandwiched between the Au electrode and a flat inner wall of a glass cell to conduct voltammetric measurements.

2.10. Electroreflectance Measurements

Potential modulation used for electroreflectance (ER) measurements is described as

$$E = E_{\text{dc}} + E_{\text{ac}} = E_{\text{dc}} + \Delta E_{\text{ac}} \exp(-j\omega t) \quad [3]$$

where E_{dc} is the dc potential, E_{ac} is the ac potential, ΔE_{ac} is the zero-to-peak ac amplitude of the potential modulation, $j = \sqrt{-1}$, and $\omega = 2\pi f$ where f is the modulation frequency. The instruments and procedures used for the ER measurements were described in our previous paper [14] and chapter [44]. The placement of the gel was the same as for the voltammetric measurements, while the gel was pressed to the inner wall of an optical window for the ER measurements.

3. Results and discussion

3.1. Optimization of viologen pendant rate

The PLLV-GA-gel samples with different ξ were examined in terms of contraction-expansion behavior, redox response in cyclic voltammograms (CVs), and spectroelectrochemical response in ER spectra. Small pieces of PLLV-GA-gel samples of $\xi = 5, 10, 25,$ and 50% were floated in the buffer solution on a slide glass plate. Immediately after addition of the dithionite solution, the color of all the gel samples began changing from faint yellow to deep purple from outside to inside. The purple color originates from $V^{\bullet+}$ and its dimer $(V^{\bullet+})_2$ as the one-electron reduction products.

Fig. 2

Table 1

The contraction of the PLLV-GA-gel samples is shown in Fig. 2 and Table 1. The gel samples with $\xi = 5\%$ and 10% did not contract despite the color change. Deformation was never observed even when the samples stayed put in the dithionite solution over 30 min. Most likely, because of the low rate of side-chain pendants, extensive GA cross-linking development between ϵ -amino groups of Lys units substantially suppressed the deformation. The 25% gel

showed greater contraction and shorter time to reach saturated contraction than the 50% gel. The 25% gel kinetically showed two-step contraction; the faster first step shifted into the slower second one when the volume became 78% of the initial state. The contraction rate in the first step for the 50% gel was faster than that for the 25% gel (Fig. S1, a plot with normalized time axis), and the 50% gel shifted to the second step earlier than the 25% gel. For the 50% gel, the presence of the very slow second step lengthened the time to reach saturated contraction. The inflection point between the first and second steps may correspond to the time point of disappearance of the non-reduced region in the gel sample, because it tends to flatten the concentration gradient of dithionite or electrons in the diffusion layer, which determines the total rate of contraction.

After saturation of contraction, re-oxidative re-expansion by the addition of O₂-saturated water was monitored. Resulting expansion was slow for both 25% and 50% gels. Hereafter in this study, we focused attention on the gels of $\xi = 25\text{-}45\%$.

Fig. 3

To evaluate electrochemical and spectroelectrochemical properties of the PLLV-GA-gel samples of different ξ , we used the results of the measurements of CVs and ER. Fig. 3 shows typical CVs at a sweep rate (ν) of 50 mV s⁻¹. The CV responses were stable at least for several hours. The midpoint potential (E_m) of the redox wave of V^{•+/2+} couple is added in Table 1. The E_m value at a Au electrode in a BCV solution was -595 mV. The E_m values for all the four gels are much less negative, indicating that reduced states of viologen are relatively stabilized in the gel. Furthermore, E_m tended to shift positively with increasing ξ . Existence of a preferential subsequent dimerization process of the reduction products or an advantageous micro-environment for reduced forms may cause the positive shift.

As far as the cathodic peak current (i_{pc}) at 50 mV s⁻¹ is concerned (Table 1), i_{pc} became greater with increasing ξ except for the 10% gel. The electron transfer kinetics in a polymer with the side-chain pendant redox groups with low concentrations is generally governed by the Brownian motion of the groups to give mutual collision, and the collision frequency per a redox unit can be lowered by more extensive cross-linking and the increase of the concentration [20]. It is also the case in the present hydrogel that the kinetics is a complex function of the cross-

linking density and the concentration of viologen sites, giving a nonlinear dependence of i_p on ξ . The gels of 10% and 50% showed i_p proportional to \sqrt{v} in the full range from 2 mV s⁻¹ to 200 mV s⁻¹, indicating that the redox reaction is apparently diffusion-controlled. In contrast, the 25%-gel and also a 40% gel showed i_p being represented by the sum of two terms, one is proportional to \sqrt{v} and the other is proportional to v . To fully understand the complex voltammetric responses, we further need to take the deformation during the measurements into account. Extensive measurements and analyses are currently underway, and the results will be reported elsewhere.

Fig. 4

Fig. 4 shows the ER spectra (ERS) of the same PLLV-GA-gel samples as those used in Fig. 3. The probe light penetrated the gel and reflected at the Au electrode surface. Because V²⁺ is colorless, the ER spectral structure is determined by two components; the major one is the light absorption by V^{•+} and its dimer (V^{•+})₂ in the gel and the minor one is the electroreflectance effect of the Au electrode surface [44,45]. Reduced forms of viologen give at least two absorption bands, one in the range of 370-400 nm and the other in the range of 530-605 nm depending on the fraction of (V^{•+})₂. The electroreflectance effect of Au gives a broad negative-going ER band with a peak at 500 nm in the real part [44]. Open diamonds in Fig. 4 mark the peaks of the Au electroreflectance band. The ERS of the 5% gel (Fig. 4-a) showed only a low-intensity Au electroreflectance signal, because the amount of viologen was small. The solid triangles in Fig. 4 mark the positions of (V^{•+})₂ band peaks. The PLLV-GA-gel samples of 25% (Fig. 1-c) and 50% (Fig. 1-d) showed a V^{•+}-dimer rich ER spectral feature. It means that the (V^{•+})₂-form dominates the reduced state of pendant viologens. The fraction of V^{•+} units in the dimer form among all V^{•+} was determined from the ER band amplitude as described in our previous publications [14,46,47]. The highest fraction of ca. 98% was found in the 25% gel sample. In the 10% samples, a peak of the monomer band was found at 600 nm (Fig. 4-b, diamond mark), indicating the relatively lower tendency of dimer formation presumably because of a lower density of viologen pendants. The relatively smaller 375 nm peak in Fig. 4-d indicates a greater effect of light scattering than in Fig. 4-c.

The results of ER measurements are in line with the CV data. The estimated concentration

of the viologen site in the swelled PLLV-GA-gel of $\xi = 25\%$ is approximately 30 mM, using the specific weight (1.0) of dry PLLV and that of dry PLLV-GA-gel (1.1) from a rough weighing and the water content of 96% [14]. In aqueous solution of short dialkyl viologens, the dimerization equilibrium constant is approximately $4 \times 10^2 \text{ M}^{-1}$, taking the firstly reported reliable value for diethyl viologen by Schwarz in the 1 M aqueous solution [48]. When using this value in the PLLV-GA-gel, an estimated fraction of viologen units in dimer among all the viologen units is calculated to be ca. 80%. The fraction obtained from ER was greater than the calculated value. Therefore, the environment in the gel or pendant configuration of the viologen units facilitates dimerization of $V^{\bullet+}$ compared to the solution phase dimerization. The positive shift of E_m also originates from the dimerization as the preferential subsequent process.

For the 10% gel, the ER signal dominating the real part was the Au electroreflectance response. For both 25% and 50% gels, the real part ER signal intensity from viologen redox was almost the same level as the imaginary part, indicating that the heterogeneous electron transfer kinetics of the gels are almost the same for the two gels.

3.2. Effects of cross-linking structure and viologen separated gel

To discuss the relevance of viologen attachment to PLL as pendant groups and cross-linking structure to the gel deformation, we prepared two gel samples in addition to PLLV-GA-gel of $\xi = 25\%$. They are a PLLV-EGDE-gel (Fig. 1-b) with $\xi = 25\%$ and a PLL-GA gel with non-bound incorporated BCV (Fig. 1-c). The PLL-GA gel + BCV (200 μM) sample was prepared by GA cross-linking of PLL followed by immersion of it in 200 μM BCV solution for 12 h and rinsing of it with a small amount of PB solution, and it was subjected to the oxidation-reduction test. The amounts of GA per Lys-unit used for cross-linking to obtain the PLLV-GA-gel and the PLL-GA gel were equal.

Reductive contraction of the PLLV-GA-gel by dithionite has been described in the previous section (Fig. 2). In contrast, no contraction was observed for the PLLV-EGDE-gel and the PLL-GA gel + BCV (200 μM). The PLL-GA gel + BCV (200 μM) did not show even any color change. Unbound BCV molecules did not remain incorporated but leaked out from the PLL-GA gel. The PLLV-EGDE-gel turned into a deep purple color without contraction, indicating that, despite the occurrence of $V^{\bullet+}$ dimer formation, neither agglomeration of the polymer

network nor water egress takes place. This may originate from rather poor Brownian motion of the side chains within EGDE linkage or rigid networking by EGDE in the exterior regions of the gel as pointed out by Bershteina et al. [22]. The flexibility of GA crosslink should be the choice rather than the rigidity of EGDE cross-linking for the redox deformation of PLLV polymer-based hydrogel. The Schiff base linkage in the GA cross-linking hydrogel was stable in repeated reduction-oxidation processes. An additional stability test in an acidic environment, which would be our due course, was not conducted because of the limitation of the sample amount.

Fig. 5

Table 2

Fig. 5 shows multiple scan CVs at $\nu = 50 \text{ mV s}^{-1}$ for the PLLV-GA-gel and the PLLV-EGDE-gel in buffer solution and the PLL-GA gel in 200 μM BCV solution. The parent PLLV for the former two gels was of $\xi = 25\%$. For comparison, the CV of a Au electrode in 300 μM BCV solution was also shown by a purple line. As shown in Table 2, the PLLV-GA-gel and the PLLV-EGDE-gel gave less negative E_m and narrower peak separations (ΔE_p) than others, indicating that attachment of viologens to the main chain relatively stabilizes the reduced form and accelerates the heterogeneous electron transfer. The CV current response of the PLLV-EGDE-gel is smaller than the PLLV-GA-gel, indicating restricted motions of the side-chain viologen units in the PLLV-EGDE-gel.

Both the PLL-GA gel + BCV (200 μM) and BCV solution showed a proportionality of i_p values to $\sqrt{\nu}$ in the ν range from 2 mV s^{-1} to 200 mV s^{-1} . The i_p values at 50 mV s^{-1} were 0.48 μA for the PLL-GA gel + BCV (200 μM) and 0.70 μA for a bare Au electrode in 300 μM BCV solution (Fig. 5), strongly suggesting that both BCV concentration and its diffusion coefficient in the swelled PLL-gel are almost the same as those in BCV solution. Because the PLLV-GA-gel with ca. 30 mM equivalent concentration of viologen units also showed the same order of i_p value, the apparent diffusion coefficient of viologen in the PLLV-GA-gel should be 4 order of magnitude smaller than the diffusion coefficient of BCV in the PLL-GA-gel. Because no long-range physical diffusion takes place in the PLLV-GA-gel, the electron transfer in it relies

on the Brownian motion-collision of the viologen units and the electron hopping between neighboring viologen units [20]. This addresses the need for the use of conductive fillers. Note that the dithionite reduction test revealed that BCV in the PLL-GA gel was washed away during rinsing and leaked out to the bathing water.

Fig. 6

Fig. 6 shows the ERS of the same samples as those used for the CV measurements in Fig. 5. The sample for Fig. 6-a was not identical to that for Fig. 4-c but showed excellent reproducibility. The real part ER signals of the PLLV-EGDE-gel (Fig. 6-b) represented mainly the Au electroreflectance signal. The imaginary parts of the PLLV-EGDE-gel represented the viologen signal of a $V^{\bullet+}$ -dimer rich feature, but the signal-to-noise ratio originating from the light scattering prevented us from estimating the dimer content. The real and imaginary parts of PLL-GA gel with permeated BCV in 200 μ M BCV (Fig. 6-c) represented approximately the half of intensity of the 300 μ M BCV solution at a bare Au electrode (Fig. 6-d). The ER spectral structure for the PLL-GA gel (Fig. 6-c) was almost the same as that of BCV solution (Fig. 6-d) and showed almost the same intensity of monomer and dimer absorption bands. An important message is that, without the covalent bonding of viologens to the polymer backbone, dimerization of $V^{\bullet+}$ is not facilitated even for the viologens in the polymer gel matrix. It is in sharp contrast to Fig. 6-a, where we found predominant $V^{\bullet+}$ -dimer absorption with only a very weak trace of $V^{\bullet+}$ -monomer. The pendant viologens can get closer as polymer chains approached each other upon reduction than unbound viologens do. The relatively smaller UV region ER response in Fig. 6-c may originate from the light scattering by the presence of the gel matrix.

3.3. Effect of incorporation of conductive filler

The conductive fillers (AuNP, GNP, and CNT) in the PLLV-GA-gel changed the time course of gel deformations as shown in Fig. 7. In this series of experiments with the fillers, we used the host PLLV of the ξ range of 35-45%, a little bit greater than that in the previous two sections, because we may gain more chance of the formation of electron transfer pathways and clearer

observation of the acceleration of the penetration of oxidation states. The initial rate of reductive contraction, defined as the average rate in the first 10 s period, was in the order of $\text{GNP} > \text{AuNP} > \text{CNT} > \text{no-filler}$ (Fig. 7-a), while the saturated contraction magnitude was in the order of $\text{no-filler} \approx \text{GNP} > \text{AuNP} > \text{CNT}$ (Fig. 7-b). The acceleration effect of conductive fillers on the initial rate is ascribable to the formation of the electron transfer pathways, the acceleration of dithionite penetration, or facilitated water egress. On the other hand, the presence of fillers showed a negative effect on the contraction limit as being pronounced by CNT. The fillers limited the contraction levels, indicating that the fillers worked as an obstacle for contraction at a certain degree.

Fig. 7

The initial rates of re-oxidative swelling of GNP and CNT gels were faster than the gel without filler for the first 100 s period after O_2 saturated water added (Fig. 7-b). The fillers made both reduction and the first stage of re-oxidation fast. Overall, the inflection point between the first and second steps of contraction came much earlier with fillers than that did without any filler. Unlike hydrophobic carbon materials, the surface of Au is hydrophilic and its adhesiveness with highly hydrophilic gel network does not allow the presence of non-contacting voids around the AuNP. Therefore, the acceleration of contraction by AuNP owes its ability of electron transfer. The main difference between the two hydrophobic nano-carbon materials is the dimension, 2D or 3D, and the latter may have advantages in the electron transfer pathway formation. Even though the same weight of CNT and GNP were used as described in the experimental section, CNT failed to reach the electron transfer in the whole bulk of the gel, being leveled at only volume shrinkage of ca. 75%

Fig. 8

Fig. 8 include CVs of the PLLV-GA-gel samples without any filler (Fig. 8-a-1, $\xi = 40\%$) and with fillers (Fig. 8 b-d). The characteristics in Fig. 8-a-1 is in line with the data of 25% gels (Figs. 3 through 6). In Fig. 8-c-1, the cathodic process of the gel with GNP was accompanied by a significant oxygen reduction current. When oxygen was bubbled, the cathodic current

increased. Removal of contaminated oxygen could not be made even by a long time of Ar gas bubbling in the solution phase. Intrinsically, graphene show high affinity of O₂ adsorption not only physically but also chemically at the graphene edges [49-51], and covalently formed surface groups also exhibit redox reaction [52]. Such a wave, however, was not observed for the CNT incorporated gel. The CV of GNP incorporated gel strongly suggests that the GNP structures near the electrode surface are electrically interconnected in the gel and some of them have firm contacts with the electrode substrate giving the O₂ reduction current.

Table 3

All the CVs showed a redox wave of V^{•+/2+} at E_m given in Table 3. Incorporation of AuNP clearly shifted E_m to less negative than E_m without fillers gel, indicating relative stabilization of the reduced form. For AuNP and CNT incorporated gels, the anodic and cathodic peak currents i_p were proportional to \sqrt{v} in the range from 2 mV s⁻¹ to 200 mV s⁻¹, indicating diffusion-controlled process. The value of i_p was in the order of AuNP > CNT \approx no-fillers. The interfacial electron transfer rate at the Au electrode surface as well as the apparent diffusion process in the gel were accelerated by AuNP. In other words, the AuNPs acted as an electron transfer pathway. For the gel with GNP, the subtraction of the contribution of O₂ reduction current could not be made immediately, but the redox current of viologen should be lower than 0.2 μ A (Fig. 8-c-1). It means that the electron transfer pathway formation by the GNP is quite limited. To its end, we may conclude that the inefficacy of nano-carbon materials to increase the current indicates that these materials only facilitate the penetration of dithionite into the gel but electron transportation acceleration is quite limited in the vicinity of the electrode or the gel external surface. Presumably, the hydrophobic conductive fillers cannot accelerate electron transfer. Although the i_p of the gel with AuNP was greater than the others, the initial rate of reductive contraction of it is not the largest. The essence of fast contraction may be not only electron transfer and penetration of dithionite but also the egress of water. To examine the egress of water, doping of polymetric anion in PLLV-GA-gel is shown in a later section.

Fig. 8 also shows the ERS of the same samples as those used for CV measurements. The gel samples except for the GNP incorporated gel showed well-defined ER spectra of the difference absorption spectral features. The bands at 540 nm and 850 nm are of the V^{•+} dimer rich reduced

state. It indicates that the fillers do not disturb $V^{\bullet+}$ dimer formation. The GNP incorporated gel showed the Au electroreflectance in the real part ERS and a complex spectral structure in the imaginary part (Fig. 8-c-2). The ERS of the GNP incorporated gel was not of the difference absorption features. No peak characteristics to $V^{\bullet+}$ species were found. Such an ER spectral structure is frequently observed for strongly adsorbed species on a solid surface [44]. Most likely, viologens strongly adsorb on the surface of GNP have produced the ER signals.

For the filler-incorporated gels, an attempt to compare the ER signal intensity should be discarded, because the light scattering and absorption by the fillers may strongly affect it. Nevertheless, the ERS still gives implications on kinetics in addition to the viologen dimer formation. At 14 Hz, a relatively greater imaginary part response was observed for AuNP incorporated gel but not for the other gels. This fact connotes the presence of multiple pathways of the propagation of the reduced state in the gel with AuNP. Further discussion should be made after optimization of the way to incorporate Au nano-structure, being now in progress in our group.

3.4. Incorporation of an anionic polymer

As described in the previous section, although all the conductive fillers accelerated initial contraction, re-oxidative swelling remained slow. The contraction and re-expansion rely on the egress and ingress of water, respectively. The movement of water driven by an osmotic pressure difference always accompanies counter anion transportation to achieve electroneutrality. To examine the replacement of the anion movements with cation movements in part, doping of an anionic polymer was tested.

To boost the penetration of water and accelerate re-oxidation swelling, we incorporated anionic polymer PSS in the PLLV-GA-gel. We used PLLV-GA-gel of $\xi = 25\%$ as the host to incorporate PSS in it. PSS in the PLLV-GA-gel electrostatically attracts both pendant V^{2+} sites and the protonated amine groups of PLL depending on pH. Even in the maximal PSS containing sample ($\xi = 25\%$ and $\varphi = 11\%$), the viologen sites is of large excess against $-SO_3^-$ of PSS, but we observed a considerable effect of poly-ion complex formation.

Fig. 9

Fig. 9 shows that the maximal contraction amplitude of all the PLLV-GA-gels with PSS was smaller than that of the PSS free PLLV-GA-gel. The initial reductive contraction rates taken as the average in the first 10 s of the gels with PSS (Fig. 9-b) were slower than that of the PSS free gel. These facts indicate that the contraction was inhibited by the presence of PSS in the gel. On the other hand, the re-oxidative swelling of PSS-incorporated gel after the saturated contraction was faster, and the swelling amplitude was greater than PSS free gel upon the addition of a saturated O₂ solution. PSS accelerated water ingress and ion uptake into the gel and made re-oxidation swelling faster in kinetics and larger in the extent.

Table 4

Fig. 9-c shows the CVs of the Au electrode with the gels with various ϕ at $\nu = 50 \text{ mV s}^{-1}$. The incorporation of PSS slightly shifted E_m (Table 4) to less negative. The value of i_p remarkably increased as a linear function of ϕ (Fig. S6). The i_p was proportional to $\sqrt{\nu}$ in the range from 2 mV s^{-1} to 200 mV s^{-1} , indicating that the redox reaction is apparently diffusion-controlled. The sharp anodic peak of the gel of $\phi = 11\%$ may result from the avalanche oxidation of viologen radical cations, indicating of poly-ion complex solid-state salt formation between $V^{\bullet+}$ and $-\text{SO}_3^-$ groups. It has been known that solid-state $V^{\bullet+}$ exhibits a sharp anodic peak [53].

The incorporation of PSS did not considerably change the value of ΔE_p (Table 4), indicating that PSS did not retard the interfacial electron transfer kinetics. Therefore, the increase of i_p with ϕ despite the constant viologen pendant amount indicates that the apparent diffusion process in the film becomes faster by PSS incorporation. This presumably originated from the shortening of the inter-viologen site average distance because of the attraction of the viologen site to PSS. At the same time, the retardation of contraction originated from the inhibition of Brownian motion of the side chain viologen sites. Taken together, the viologen sites adhered electrostatically to PSS chain, and on one hand the movements are restricted but on the other hand more chance is given to viologen sites stay in close distances to facilitate bimolecular electron hopping. Because the maximal ϕ was 11%, effect of the much faster mobility of K^+ in the gel is improbable to be unveiled if any.

The ERS of the same PLLV-GA-gel with PSS used for CV measurements are shown in Fig. S7. The gel with $\phi = 30\%$ looked so noisy as to significantly scatter the probe light, discarding the applicability of the ER method. The ERS of the gel of $\phi = 1.1\%$ and $\phi = 5.7\%$ had viologen dimer bands at 370 nm and 535 nm. The presence of PSS does not prevent viologens from forming dimers. But the heterogeneous electron transfer rate with the Au electrode of the gel of $\phi = 1.1\%$ was slightly faster than the gel of $\phi = 5.7\%$, because redox response in the imaginary part of the ER signal for the 5.7% gel was lost.

4. Conclusion

The deformation and electrochemistry of a viologen-incorporated polymer hydrogel, PLLV-GA-gel, was investigated. As the actuation polymer gel constituents, the polymer in the gel is quite unique in the way to use of viologen sites as side-chain pendants but not in the polymer main-chain backbone. The research into the direction to enhance the redox driven deformation of the PLLV-GA-gel unveiled the following points:

- i) The greatest volume change upon reductive contraction was attained with a 25% pendant rate sample.
- ii) Incorporation of conductive fillers, AuNP, GNP, and CNT, accelerated the initial contraction rate but appeared ineffective in the acceleration of re-oxidative expansion.
- iii) Incorporation of a small amount of an anionic polymer, PSS, resulted in the partial formation of poly-ion complex with viologen and ammonium sites and showed a significant change of the deformation and voltammogram; it accelerated the initial re-oxidative expansion but slowed down the contraction, while it largely enhanced the voltammetric response.
- iv) The cross-linking agent should be flexible enough to allow active Brownian motion of the side chains.
- v) The apparent diffusion coefficient of pendant viologens in the PLLV-GA-gel is 4 order of magnitude smaller than that of free BCV.
- vi) The $V^{\bullet+}$ -dimer formation is indispensable for the deformability.

Although the direction of the improvements was newly shed light in this work, we cannot

reach the tentative target levels of deformation. An important observation in this experimental work is the fact that, although the floating PLLV-GA-gel, whichever it contains a filler or polyanion, can be reduced completely to the center of the sample piece by dithionite, a complete potentiostatic reduction for ca. 2 mm-thick sandwiched gel on the electrode surface required hours of time. This reveals that the electron hopping pathway is not extended over the gel bulk but restricted to the part even in the presence of fillers. The PLLV-GA-gel itself does not have any conjugated electron-conductive network. One of the resolutions may be blending a conductive polymer [4] but the frequently used conductive polymers are in insulating state at the potentials which should be applied to reduce viologen sites. Photo-induced reduction of viologens to lead the gel conduction is an excellent strategy as demonstrated by Barnes and coworkers [16-18], while our direction is the deformation on an electrode even in the dark. We are now underway to incorporate a better conductor network without giving any obstacle to the deformation. Furthermore, it is indispensable to understand the properties of the gel with fillers, and we are in preparation of microscopic measurements such as polarization or fluorescence optical microscope and electron microscopes.

Acknowledgements

This work was supported by a Grant-in Aid for Scientific Research on Innovative Areas “Molecular Engine” (JSPS KAKENHI Grant JP19H05400) to T.S.

References

- [1] K. Kaneto, Research Trends of Soft Actuators based on Electroactive Polymers and Conducting Polymers, *J. Phys.: Conf. Ser.* 704 (2016) 012004: 1-9.
<https://doi.org/10.1088/1742-6596/704/012004>
- [2] F. Hu, Y. Xue, J. Xu, B. Lu, PEDOT-Based Conducting Polymer Actuators, *Front. Robot. AI* 6 (2019) 114: 1-17. <https://doi.org/10.3389/frobt.2019.00114>
- [3] S. Maeda, Y. Hara, T. Sakai, R. Yoshida, S. Hashimoto, Self-Walking Gel, *Adv. Mater.* 19 (2007) 3480–3484. <https://doi.org/10.1002/adma.200700625>
- [4] L.-M. Low, S. Seetharaman, K.-Q. He, M.J. Madou, Microactuators toward microvalves for responsive controlled drug delivery, *Sens. Actuators B Chem.* 67 (2000) 149-160.
[https://doi.org/10.1016/S0925-4005\(00\)00396-8](https://doi.org/10.1016/S0925-4005(00)00396-8)
- [5] K. Kaneto, M. Kaneko, Y. Min, A. G. MacDiarmid, “Artificial muscle”: Electromechanical actuators using polyaniline films, *Synth. Met.* 71 (1995) 2211-2212.
[https://doi.org/10.1016/0379-6779\(94\)03226-V](https://doi.org/10.1016/0379-6779(94)03226-V)
- [6] S. Han, C. Liu, X. Lin, J. Zheng, J. Wu, C. Liu, Dual Conductive Network Hydrogel for a Highly Conductive, Self-Healing, Anti-Freezing, and Non-Drying Strain Sensor, *ACS Appl. Polym. Mater.* 2 (2020) 996–1005. <https://doi.org/10.1021/acsapm.9b01198>
- [7] T. Tatsuma, K. Takada, H. Matsui, N. Oyama, A Redox Gel. Electrochemically Controllable Phase Transition and Thermally Controllable Electrochemistry, *Macromolecules* 27 (1994) 6687–6689. <https://doi.org/10.1021/ma00100a067>
- [8] M.A. Hempenius, C. Cirimi, F.L. Savio, J. Song, G.J. Vancso, Poly(ferrocenylsilane) Gels and Hydrogels with Redox-Controlled Actuation, *Macromol. Rapid Commun.* 31 (2010) 772–783. <https://doi.org/10.1002/marc.200900908>
- [9] A. Akhoury, L. Bromberg, T.A. Hatton, Redox-Responsive Gels with Tunable Hydrophobicity for Controlled, Solubilization and Release of Organics, *ACS Appl. Mater. Interfaces* 3 (2011) 1167–1174. <https://doi.org/10.1021/am200002b>
- [10] M. Nakahata, Y. Takashima, A. Hashidzume, A. Harada, Redox-Generated Mechanical Motion of a Supramolecular Polymeric Actuator Based on Host–Guest Interactions, *Angew. Chem. Int. Ed.* 52 (2013) 5731–5735. <https://doi.org/10.1002/anie.201300862>
- [11] M. Nakahata, Y. Takashima, A. Harada, Redox-Responsive Macroscopic Gel Assembly Based on Discrete Dual Interactions, *Angew. Chem. Int. Ed.* 53 (2014) 3617–3621.

- <https://doi.org/10.1002/anie.201310295>
- [12] N. Hisamatsu, T. Iida, T. Yasui, K. Takada, A. Yuchi, Double-side Coated Electrochemical Actuator Based on Changes in Volume of Poly(acrylic Acid) Gel, *Sens. Actuators B Chem.* 203 (2014) 289–295. <https://doi.org/10.1016/j.snb.2014.06.123>
- [13] K. Takada, T. Iida, Y. Kawanishi, T. Yasui, A. Yuchi, An Electrochemical Actuator Based on Reversible Changes in Volume of Poly(acrylic Acid) Gel Induced by Quinone Redox, *Sens. Actuators B Chem.* 160 (2011) 1586–1592. <https://doi.org/10.1016/j.snb.2011.09.031>
- [14] B. Wang, H. Tahara, T. Sagara, Driving Quick and Large Amplitude Contraction of Viologen-Incorporated Poly-L-Lysine based Hydrogel by Reduction, *ACS Appl. Mater. Interfaces* 10 (2018) 36415–36424. <https://doi.org/10.1021/acsami.8b12530>
- [15] A.F. Greene, M.K. Danielson, A.O. Delawder, K.P. Liles, X. Li, A. Natraj, A. Wellen, J.C. Barnes, Redox-Responsive Artificial Molecular Muscles: Reversible Radical-Based Self-Assembly for Actuating Hydrogels, *Chem. Mater.* 29 (2017) 9498–9508. <https://doi.org/10.1021/acs.chemmater.7b03635>
- [16] K.P. Liles, A.F. Greene, M.K. Danielson, N.D. Colley, A. Wellen, J.M. Fisher, J.C. Barnes, Photoredox - Based Actuation of an Artificial Molecular Muscle, *Macromol. Rapid Commun.* 39 (2018) 1700781. <https://doi.org/10.1002/marc.201700781>
- [17] F. Amir, K.P. Liles, A.O. Delawder, N.D. Colley, M.S. Palmquist, H.R. Linder, S.A. Sell, J.C. Barnes, Reversible Hydrogel Photopatterning: Spatial and Temporal Control over Gel Mechanical Properties Using Visible Light Photoredox Catalysis, *ACS Appl. Mater. Interfaces* 11 (2019) 24627–24638. <https://doi.org/10.1021/acsami.9b08853>
- [18] A.O. Delawder, A. Natraj, N.D. Colley, T. Saak, A.F. Greene, J.C. Barnes, Synthesis, self-assembly, and photomechanical actuator performance of a sequence-defined polyviologen crosslinker, *Supramol. Chem.* 31 (2019) 523–531. <https://doi.org/10.1080/10610278.2019.1632453>
- [19] F. Amir, X. Li, M.C. Gruschka, N.D. Colley, L. Li, R. Li, H.R. Linder, S.A. Sell, J. Barnes, Dynamic, multimodal hydrogel actuators using porphyrin-based visible light photoredox catalysis in a thermoresponsive polymer network, *Chem. Sci.* 11 (2020) 10910–10920. <https://doi.org/10.1039/D0SC04287K>

- [20] K. Sato, R. Ichinoi, R. Mizukami, T. Serikawa, Y. Sasaki, J. Lutkenhaus, H. Nishide, K. Oyaizu, Diffusion-Cooperative Model for Charge Transport by Redox-Active Nonconjugated Polymers, *J. Am. Chem. Soc.* 140 (2017) 1049-1056.
<https://doi.org/10.1021/jacs.7b11272>
- [21] R. Rodriguez, C. Alvarez-Lorenzo, A. Concheiro, Cationic cellulose hydrogels: kinetics of the cross-linking process and characterization as pH-/ion-selective drug delivery systems, *J. Control. Release* 86 (2003) 253-265.
[https://doi.org/10.1016/S0168-3659\(02\)00410-8](https://doi.org/10.1016/S0168-3659(02)00410-8)
- [22] V.A. Bershteina, L.M. Egorovaa, P.N. Yakusheva, P. Syselb, R. Hobzovab, J. Kotekb, P. Pissisc, S. Kripotouc, P. Maroulasca, Hyperbranched polyimides crosslinked with ethylene glycol diglycidylether: Glass transition dynamics and permeability, *Polymer* 47 (2006) 6765-6772. <http://doi:10.1016/j.polymer.2006.07.056>
- [23] H. Guo, Y. Liu, Y. Yang, G. Wu, K. Demella, S.R. Raghavan, Z. Nie, A shape-shifting composite hydrogel sheet with spatially patterned plasmonic nanoparticles, *J. Mater. Chem. B* 7 (2019) 1679-1683. <https://doi.org/10.1039/c8tb01959b>
- [24] K. Onishi, S. Sewa, K. Asaka, N. Fujiwara, K. Oguro, Morphology of electrodes and bending response of the polymer electrolyte actuator, *Electrochim. Acta* 46 (2001) 737-743. [https://doi.org/10.1016/S0013-4686\(00\)00656-3](https://doi.org/10.1016/S0013-4686(00)00656-3)
- [25] K. Onishi, S. Sewa, K. Asaka, N. Fujiwara, K. Oguro, The effects of counter ions on characterization and performance of a solid polymer electrolyte actuator, *Electrochim. Acta* 46 (2001) 1233-1241. [https://doi.org/10.1016/S0013-4686\(00\)00695-2](https://doi.org/10.1016/S0013-4686(00)00695-2)
- [26] M. Park, H. Chang, D.-H. Jeong, J. Hyun, Spatial deformation of nanocellulose hydrogel enhances SERS, *BioChip J.* 7 (2013) 234-241.
<https://doi.org/10.1007/s13206-013-7306-5>
- [27] J. Cai, X. Zhang, W. Liu, J. Huang, X. Qiu, Synthesis of highly conductive hydrogel with high strength and super toughness, *Polymer* 202 (2020) 122643: 1-9.
<https://doi.org/10.1016/j.polymer.2020.122643>
- [28] Q. Guan, G. Lin, Y. Gong, J. Wang, W. Tan, D. Bao, Y. Liu, Z. You, X. Sun, Z. Wen, Y. Pan, Highly efficient self-healable and dual responsive hydrogel-based deformable triboelectric nanogenerators for wearable electronics, *J. Mater. Chem. A* 7 (2019) 13948-13955. <https://doi.org/10.1039/c9ta02711d>

- [29] J.-T. Lee, J. Lee, Y. Kwon, J.-Y. Kim, Y. Lin, Y.-H. Lee, S.-R. Paik, Ultra-thin free-floating carbon nanotube/gold nanoparticle hybrid film prepared with self-assembly protein of α -synuclein, *Sens. actuators B Chem.* 305 (2020) 127514: 1-8.
<https://doi.org/10.1016/j.snb.2019.127514>
- [30] L.-Y. Hsiao, L. Jing, K. Li, H. Yang, Y. Li, P.-Y. Chen, Carbon nanotube-integrated conductive hydrogels as multifunctional robotic skin, *Carbon* 161 (2020) 784-793.
<https://doi.org/10.1016/j.carbon.2020.01.109>
- [31] H. Wang, S.K. Biswas, S. Zhu, Y. Lu, Y. Yu, J. Han, X. Xu, Q. Wu, H. Xiao, Self-Healable Electro-Conductive Hydrogels Based on Core-Shell Structured Nanocellulose/Carbon Nanotubes Hybrids for Use as Flexible Supercapacitors, *Nanomaterials* 10 (2020) 112: 1-21. <https://doi.org/10.3390/nano10010112>
- [32] Z. Qin, X. Sun, Q. Yu, H. Zhang, X. Wu, M. Yao, W. Liu, F. Yao, J. Li, Carbon Nanotubes/Hydrophobically Associated Hydrogels as Ultrastretchable, Highly Sensitive, Stable Strain, and Pressure Sensors, *ACS Appl. Mater. Interfaces* 12 (2020) 4944–4953.
<https://doi.org/10.1021/acsami.9b21659>
- [33] F. Gao, H. Teng, J. Song, G. Xua, X. Luo, A flexible and highly sensitive nitrite sensor enabled by interconnected 3D porous polyaniline/carbon nanotube conductive hydrogels, *Anal. Methods* 12 (2020) 604-610. <https://doi.org/10.1039/C9AY02442E>
- [34] J. Chen, H. Wen, G. Zhang, F. Lei, Q. Feng, Y. Liu, X. Cao, H. Dong, Multifunctional Conductive Hydrogel/Thermochromic Elastomer Hybrid Fibers with a Core–Shell Segmental Configuration for Wearable Strain and Temperature Sensors, *ACS Appl. Mater. Interfaces* 12 (2020) 7565-7574. <https://doi.org/10.1021/acsami.9b20612>
- [35] F. He, X. You, H. Gong, Y. Yang, T. Bai, W. Wang, W. Guo, X. Liu, M. Ye, Stretchable, Biocompatible, and Multifunctional Silk Fibroin-Based Hydrogels toward Wearable Strain/Pressure Sensors and Triboelectric Nanogenerators, *ACS Appl. Mater. Interfaces* 12 (2020) 6442–6450. <https://doi.org/10.1021/acsami.9b19721>
- [36] N. Yang, C.G. Zoski, Polymer Films on Electrodes: Investigation of Ion Transport at Poly(3,4-ethylenedioxythiophene) Films by Scanning Electrochemical Microscopy, *Langmuir* 22 (2006) 10338-10347. <https://doi.org/10.1021/la061167u>
- [37] A. Lisowska-Oleksiak, K. Kazubowska, A. Kupniewska, Ionic transport of Li^+ in polymer films consisting of poly(3,4-ethylenedioxythiophene) and poly(4-styrenesulphonate), *J.*

- Electroanal. Chem. 501 (2001) 54-61. [https://doi.org/10.1016/S0022-0728\(00\)00480-0](https://doi.org/10.1016/S0022-0728(00)00480-0)
- [38] O.L. Gribkova, A.A. Nekrasov, V.F. Ivanov, V.I. Zolotarevsky, A.V. Vannikov, Templating effect of polymeric sulfonic acids on electropolymerization of aniline, *Electrochim. Acta* 122 (2014) 150-158. <https://doi.org/10.1016/j.electacta.2013.12.025>
- [39] X. Ren, P.G. Pickup, Impedance spectroscopy of polypyrrole/poly(styrenesulphonate) composites. Simultaneous anion and cation transport, *Electrochim. Acta* 41 (1996) 1877-1882. [https://doi.org/10.1016/0013-4686\(95\)00507-2](https://doi.org/10.1016/0013-4686(95)00507-2)
- [40] R. Myoungcho, Surface Roughness Changes of Poly(N-Methylpyrrole)/Poly(Styrene Sulfonate) with Doping in Perchlorate Solutions of Various Cations, *J. Electrochem. Soc.* 152 (2005) E90. <https://iopscience.iop.org/article/10.1149/1.1856989/meta>
- [41] J. Migdalski, T. Blaz, A. Lewenstam, Inducing Cationic Sensitivity of Polypyrrole Films Doped with Metal Complexing Ligands by Chemical and Electrochemical Methods, *Chemica Analityczna (Warsaw, Poland)* 47 (2002) 371-384.
<http://beta.chem.uw.edu.pl/chemanal/PDFs/2002/CHAN2002V47P00371.pdf>
- [42] M. Morita, S. Miyazaki, M. Ishikawa, Y. Matsuda, H. Tajima, K. Adachi, F. Anan, Layered Polyaniline Composites with Cation - Exchanging Properties for Positive Electrodes of Rechargeable Lithium Batteries, *J. Electrochem. Soc.* 142 (1995) L3-L5.
<https://iopscience.iop.org/article/10.1149/1.2043981>
- [43] Y. Zhang, H. Yin, Y. Feng, Oppositely Charged Polyelectrolyte Complexes for High-Salinity Hydrofracking Fluid, *Ind. Eng. Res.* 58 (2019) 18488-164987.
<https://doi.org/10.1021/acs.iecr.9b03170>
- [44] T. Sagara, UV-visible Reflectance Spectroscopy of Thin Organic Films at Electrode Surfaces, In: C. Alkire, D.M. Kolb, J. Lipkowski, P.N. Ross (Eds), *Advances in Electrochemical Science and Engineering*, Vol. 9, Eds. Wiley-VCH Verlag, Weinheim, 2006, pp. 47-95.
- [45] J.D.E. McIntyre, in: R. H. Müller (Ed.), *Advances in Electrochemistry and Electrochemical Engineering*, Vol. 9, John Wiley and Sons, (1973) Chap. 2.
- [46] T. Sagara, N. Kaba, M. Komatsu, M. Uchida, N. Nakashima, Estimation of Average Orientation of Surface-Confined Chromophores on Electrode Surfaces Using Electroreflectance Spectroscopy, *Electrochim. Acta* 43 (1998) 2183-2193.
[https://doi.org/10.1016/S0013-4686\(97\)10100-1](https://doi.org/10.1016/S0013-4686(97)10100-1)

- [47] T. Sagara, H. Maeda, Y. Yuan, N. Nakashima, Voltammetric and Electroreflectance Study of Thiol-Functionalized Viologen Monolayers on Polycrystalline Gold: Effect of Anion Binding to a Viologen Moiety, *Langmuir* 15 (1999) 3823-3830.
<https://doi.org/10.1021/la9900472>
- [48] E.M. Kosower, J.L. Cotter, Stable free radicals. II. The reduction of 1-Methyl-4-cyanopyridinium ion to methylviologen cation radical, *J. Am. Chem. Soc.* 86 (1964) 5524-5527.
- [49] J. Angel Mene'ndez, B. Xia, J. Phillips, L.R. Radovic, On the Modification and Characterization of Chemical Surface Properties of Activated Carbon: Microcalorimetric, Electrochemical, and Thermal Desorption Probes, *Langmuir* 13 (1997) 3414-3421.
<https://doi.org/10.1021/la970200x>
- [50] G.J. Soldano, M.F. Juarez, B.W.T. Teo, E. Santos, Structure and stability of graphene edges in O₂ and H₂ environments from ab initio thermodynamics, *Carbon* 78 (2014) 181-189. <http://dx.doi.org/10.1016/j.carbon.2014.06.070>
- [51] B. Náfrádi, M. Choucair, P.D. Southon, C.J. Kepert, L. Forró, Strong Interplay between the Electron Spin Lifetime in Chemically Synthesized Graphene Multilayers and Surface-Bound Oxygen, *Chem. Eur. J.* 21 (2015) 770-777.
<https://doi.org/10.1002/chem.201404309>
- [52] R.L. McCreery, Carbon electrodes: structural effects on electron transfer kinetics, in: A. Bard (Ed.) *Electroanalytical Chemistry*, vol. 17, Dekker, New York, (1991) pp. 221-373.
- [53] H.-X. Wang, T. Sagara, H. Sato, K. Niki, Electroreflectance study of redox reaction of heptylviologen at a silver electrode *J. Electroanal. Chem.* 331 (1992) 925-943.
[https://doi.org/10.1016/0022-0728\(92\)85015-U](https://doi.org/10.1016/0022-0728(92)85015-U)

Table 1

Pendant rate dependence of maximum contraction volume, time period to saturated contraction, and characteristic of CV and ER for PLLV-GA-gel.

ξ (%)	5	10	25	50
Max. volume contraction (%)	0	0	97	87
Time to saturated contraction (s)	N.A.	N.A.	300	1500
E_m / mV in CV at 50 mV s ⁻¹	-500	-434	-453	-439
i_{pc} / μ A in CV at 50 mV s ⁻¹	-0.13	-0.44	-0.32	-0.62
V ⁺ -dimer content from ER (%)	N.A.	dimer predominant	98	88

N.A.: not available

Table 2

Volume contraction, time period to saturated contraction, and characteristic of CV and ER for PLLV-GA-gel and PLLV-EGDE-gel, PLL-GA + BCV (200 μ M), and BCV (300 μ M) solution at a Au electrode.

Samples	PLLV- GA-gel	PLLV- EGDE-gel	PLL-GA + BCV	BCV
Max. volume contraction (%)	93	0	0	-
Time to saturated contraction (s)	300	N.A.	N.A.	-
E_m / mV in CV at 50 mV s ⁻¹	-457	-490	-592	-595
Peak separation ΔE_p / mV	22	24	65	53
V ⁺ -dimer content from ER (%)	98	dimer predominant	83	60

ΔE_p was taken from the CV at $v = 2$ mV s⁻¹

Table 3

Properties of PLLV-GA-gel with conductive fillers.

Filler	None	AuNP	GNP	CNT
ξ	40%	35%	35%	40%
Max. volume contraction (%)	-	92	97	75
Time to saturated contraction (s)	-	200	161	200
E_m / mV (CV at 50 mV s ⁻¹)	-441	-398	ca. -404	-440
ΔE_p / mV	29	33	N.A.	26

 ΔE_p was taken from the CV at $v = 2$ mV s⁻¹**Table 4**The Effect of PSS incorporation in a PLLV-GA-gel of $\xi = 25\%$ on the contraction behavior and CV response.

ϕ	0%	1.1%	5.7%	11%
Max. volume contraction (%)	97	80	61	69
Time to saturated contraction (s)	300	180	165	143
E_m / mV (CV at 50 mV s ⁻¹)	-453	-455	-436	-431
ΔE_p / mV	22	20	~0	42

 ΔE_p was taken from the CV at $v = 2$ mV s⁻¹

Figure captions

Fig. 1. Structures of hydrogel samples: (a) PLLV-GA-gel, (b) PLLV-EGDE-gel, (c) PLL-GA gel with unbound BCV. PLLV: poly-L-lysine with pendant viologen sites, GA: glutaraldehyde as a cross-linker, EGDE: ethylene glycol diglycidyl ether as a cross-linker, PLL-GA: GA cross-linked poly-L-lysine based hydrogel, BCV: 1-benzyl-1'-(7-carboxyheptyl)-4,4'-bipyridinium dibromide.

Fig. 2. Plot of relative volume change with time for floating PLLV-GA-gel samples (ca. 2 mm or smaller) with various ξ , noted to each line, upon reduction by excess dithionite and following reoxidation by excess O_2 . The arrows indicate switching points from reduction to oxidation. For details, see section 2.8.

Fig. 3. Cyclic voltammograms (CVs) of PLLV-GA-gel with various ξ , noted to each line, in contact with a Au electrode (0.020 cm^2) in PB solution ($\text{pH} = 7.0$) at $\nu = 50 \text{ mV s}^{-1}$. The cross-marks in the CV charts show the position of zero-potential and zero-current. Sweep rate dependence of CV peak current is shown in Fig. S2.

Fig. 4. ER spectra of a Au electrode in contact with a piece of PLLV-GA-gel in PB solution. Potential modulation, $70 \text{ mV}_{\text{rms}}$ at a frequency of 14 Hz with $E_{\text{dc}} = E_{\text{m}}$. (a) $\xi = 5\%$, (b) $\xi = 10\%$, (c) $\xi = 25\%$, and (d) $\xi = 50\%$. The Au electroreflectance response (\diamond), $V^{\bullet+}$ monomer bands (\blacklozenge) at 401 nm and 603 nm, and $V^{\bullet+}$ dimer bands (\blacktriangle) at 371 nm, 533 nm, and $\sim 860 \text{ nm}$ are marked.

Fig. 5. CVs of the hydrogel samples, PLLV-GA-gel (green line) and PLLV-EGDE-gel (blue line), in contact with a Au electrode in PB solution, and PLL-GA gel in contact with an entire surface of the Au electrode immersed in buffered 200 μM BCV solution (gray line). CV at a bare Au electrode in buffered 300 μM BCV solution (purple line) was also added. The cross-marks in the CV charts show the position of zero-potential and zero-current. Sweep rate dependence of CV peak current is shown in Fig. S3.

Fig. 6. ER spectra of a Au electrode in contact with a piece of PLLV hydrogel. Potential

modulation, $70 \text{ mV}_{\text{rms}}$ at a frequency of 14 Hz with $E_{\text{dc}} = E_{\text{m}}$. (a) newly prepared PLLV-GA-gel, (b) PLLV-EGDE-gel, (c) PLL-GA-gel in $200 \mu\text{M}$ BCV, and (d) $300 \mu\text{M}$ BCV solution. $V^{\bullet+}$ monomer band (\blacklozenge): 401 nm and 603 nm, $V^{\bullet+}$ dimer band (\blacktriangle): 371 nm, 533 nm, and ~ 860 nm are marked in the spectra.

Fig. 7. Plot of relative volume change with time for floating PLLV-GA-gel samples (ca. 2 mm or smaller) without filler (w/o filler, red solid circle) and with fillers, noted to each line, upon reduction by excess dithionite and following reoxidation by excess O_2 . For ξ -values for the parent gels, see Table 3. The base solution was PB solution. Part a shows first 50 s after addition of dithionite, and part b shows full courses. The arrows indicate switching points from reduction to oxidation.

Fig. 8. CVs and ERS of the PLLV-GA-gel without filler (a) and with fillers (b: AuNP, c: GNP, d: CNT) in contact with a Au electrode in PB solution. The cross-marks in the CV charts show the position of zero-potential and zero-current. Sweep rate dependence of CV peak current is shown in Fig. S4. Potential modulation for ER measurements: $70 \text{ mV}_{\text{rms}}$ at a frequency of 14 Hz with $E_{\text{dc}} = E_{\text{m}}$. The marks in ERS have the same meanings as those in Fig. 4.

Fig. 9. Relative volume change with time (parts a and b) and CV of PLLV-GA-gel ($\xi = 25\%$) with and without PSS incorporation. Part a: plot of relative volume change with time, the first 100 s upon reduction by excess dithionite, Part b: the same plot as a but for full time courses. The arrows indicate switching points from reduction to oxidation. Part c: CV of the PLLV-GA-gels in contact with a Au electrode in PB solution. The cross-marks in the CV charts show the position of zero-potential and zero-current. Sweep rate dependence of CV peak current is shown in Fig. S5.

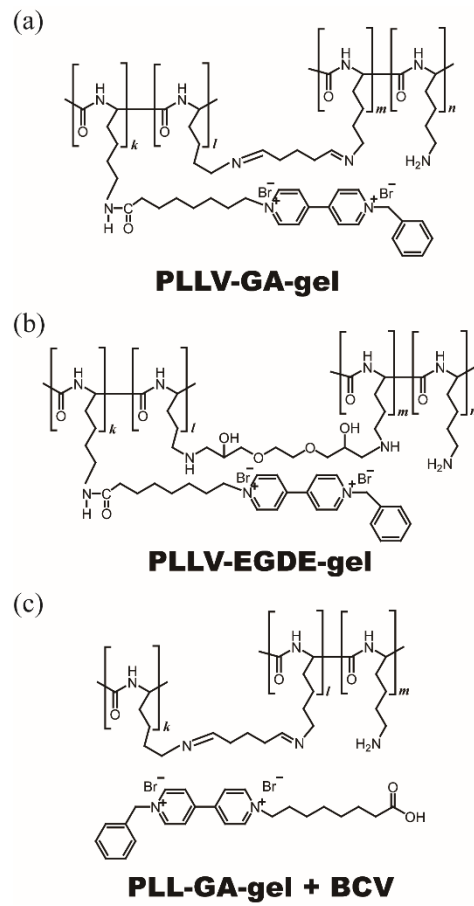


Fig. 1

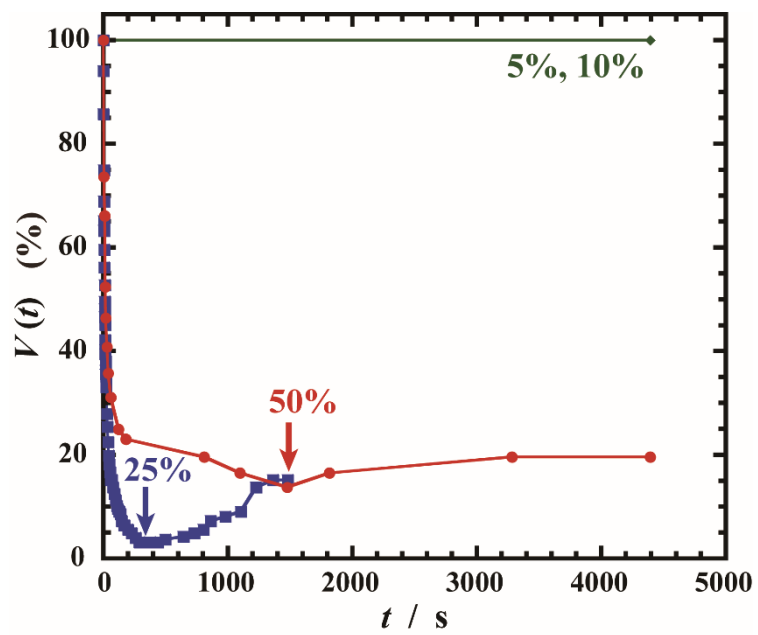


Fig. 2

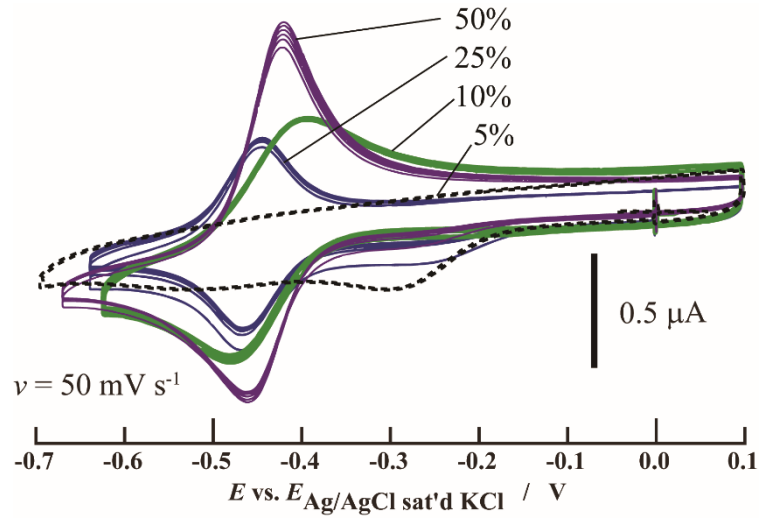


Fig. 3

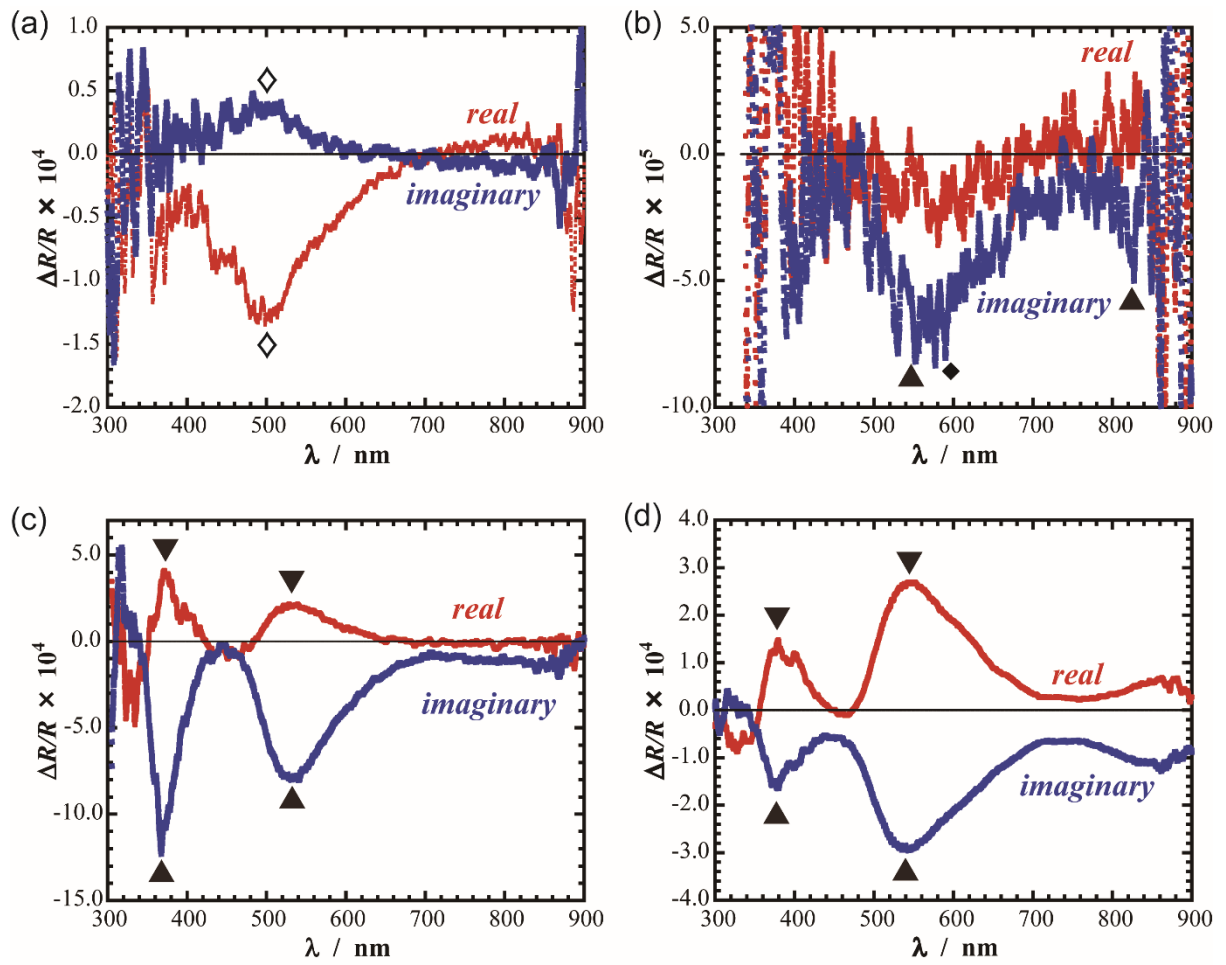


Fig. 4

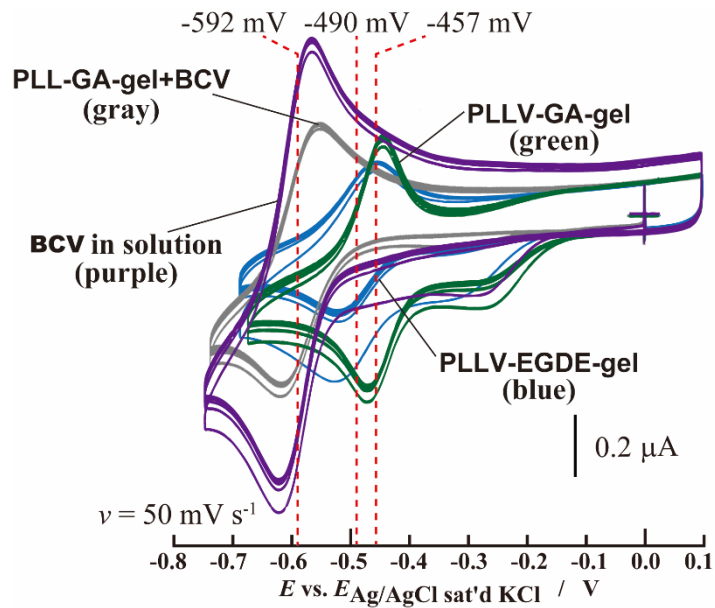


Fig. 5

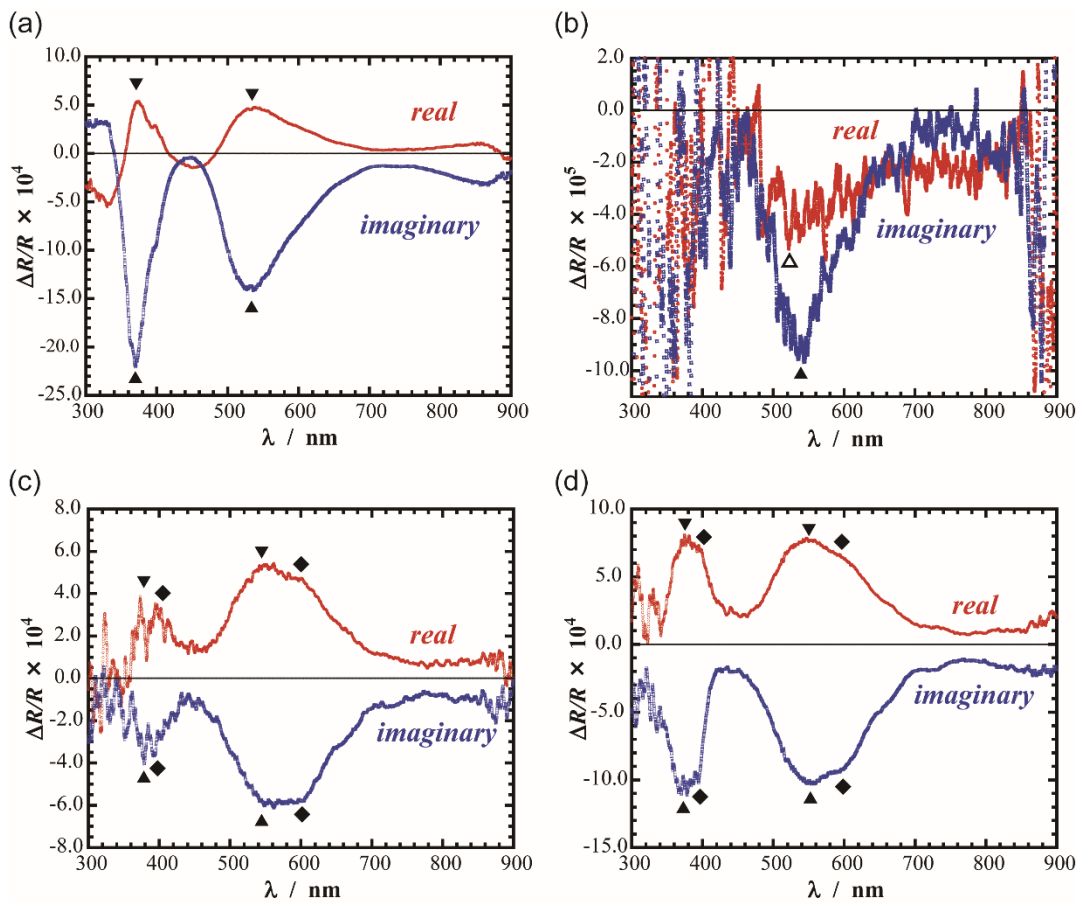


Fig. 6

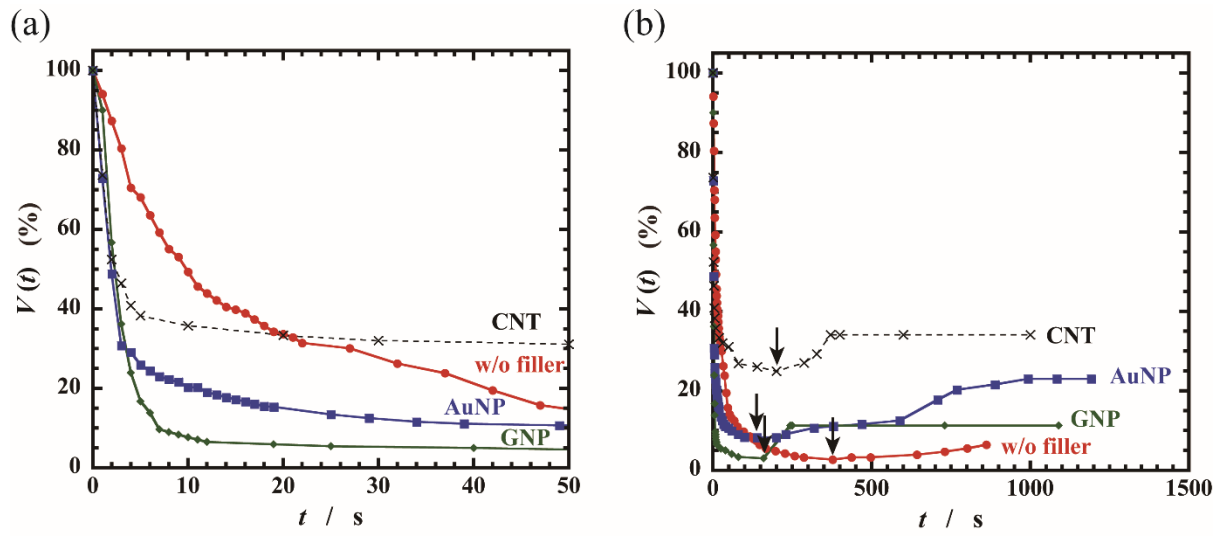


Fig.7

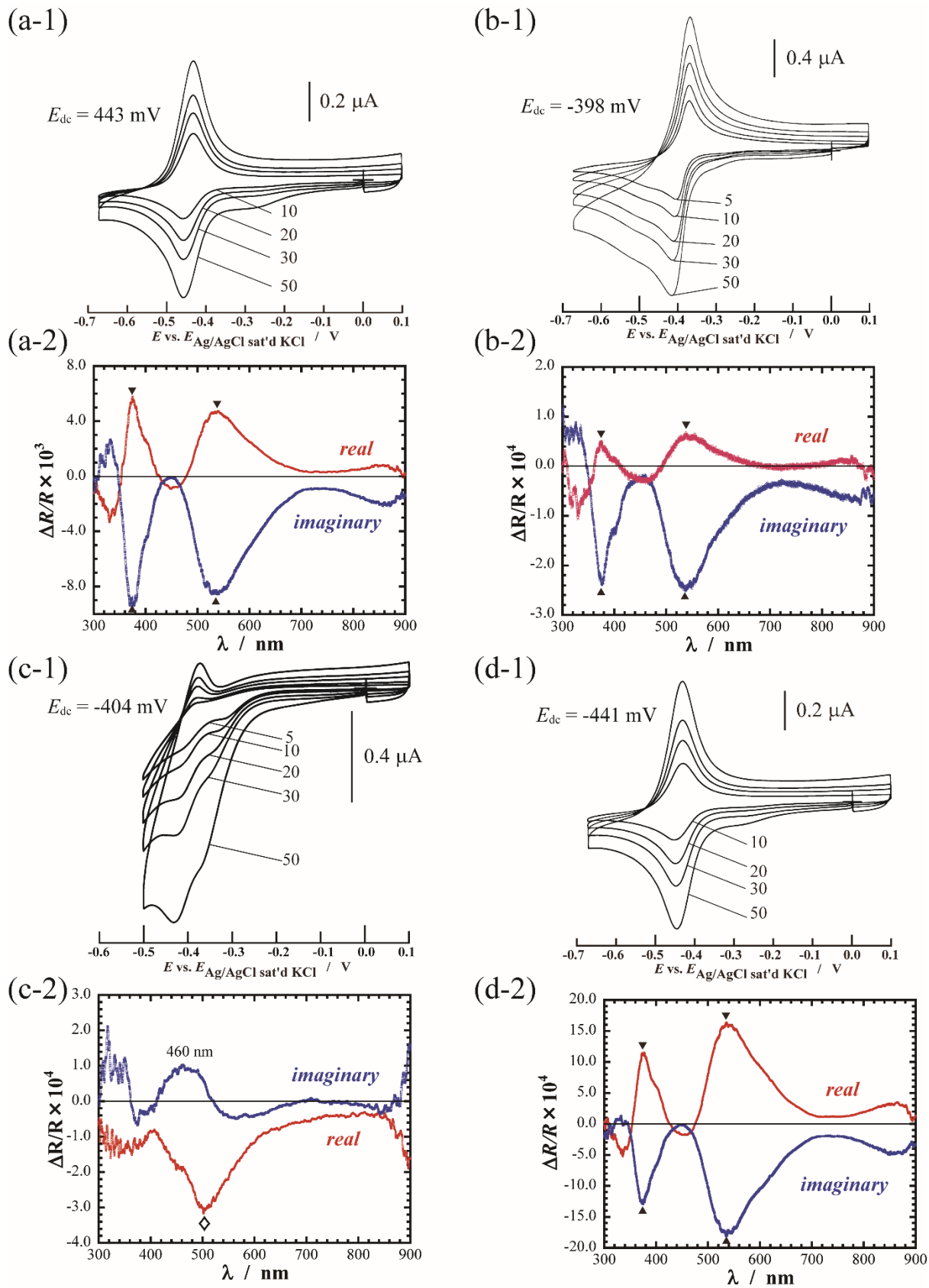


Fig. 8

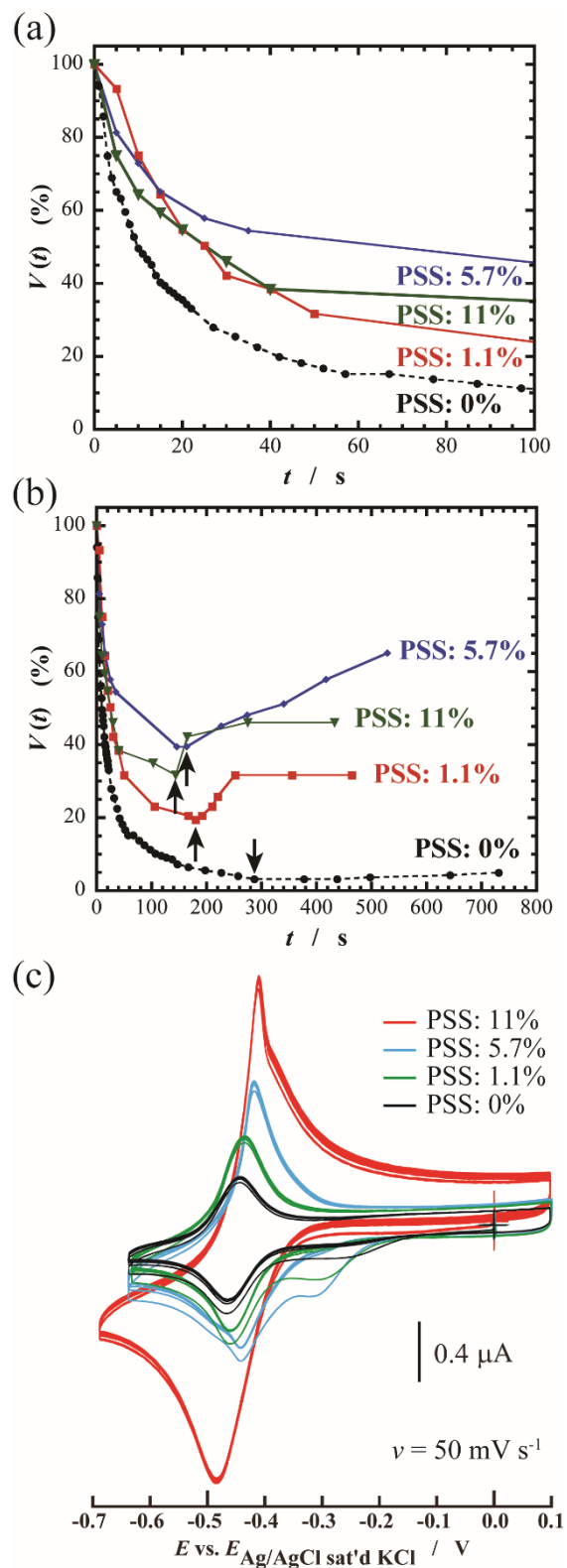


Fig. 9

Supporting Information

Enhancement of deformation of redox-active hydrogel as an actuator by increasing pendant viologens and adding filler or counter-charged polymer

Bo Wang^a, Hironobu Tahara^b, Takamasa Sagara^{b,*}

^a *Department of Advanced Technology and Science for Sustainable Development, Graduate School of Engineering, Nagasaki University, Nagasaki 852-8521, Japan*

^b *Division of Chemistry and Materials Science, Graduate School of Engineering, Nagasaki University, Bunkyo 1-14, Nagasaki 852-8521, Japan*

* Corresponding author

E-mail address sagara@nagasaki-u.ac.jp

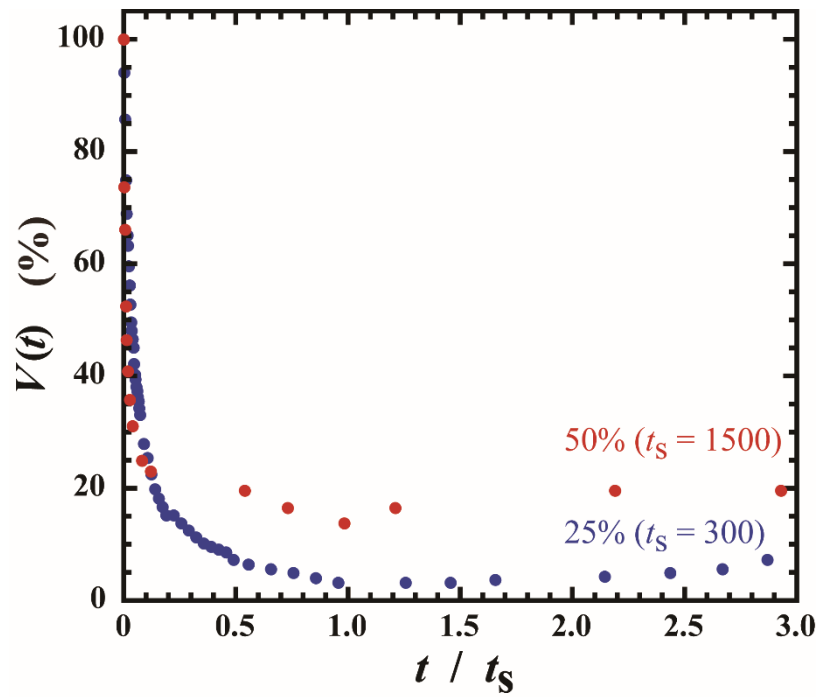


Fig. S1. Plot of time course of the relative volume of the PLLV-GA-gels with $\xi = 25\%$ and 50 % using a normalized time abscissas axis, where t_s is the time to reach saturated contraction.

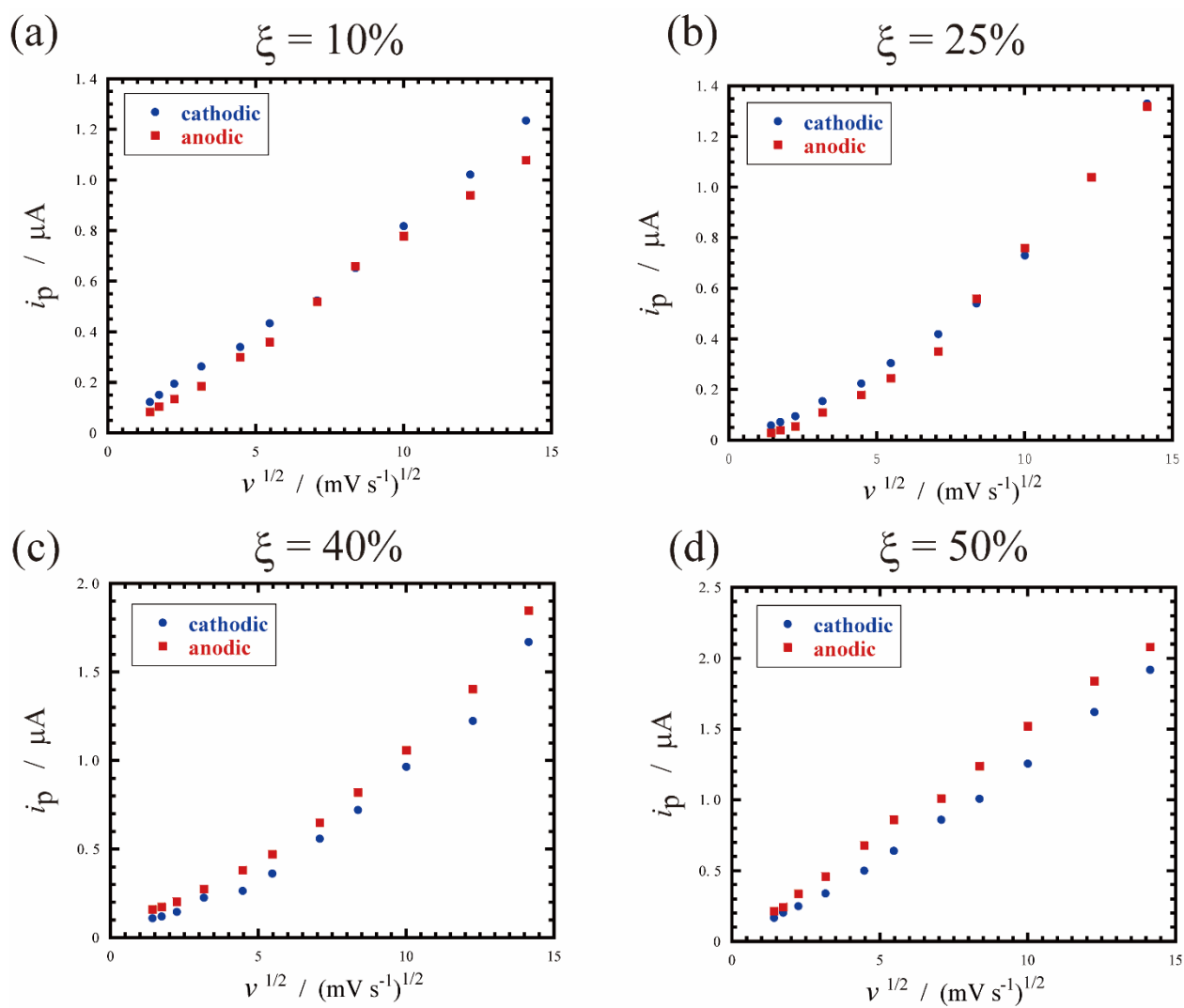


Fig. S2. Peak current vs. scan rate depend on viologen pendant rate $\xi = 10$ (a), 25 (b), 40 (c), 50 (d). See Fig. 3 for details.

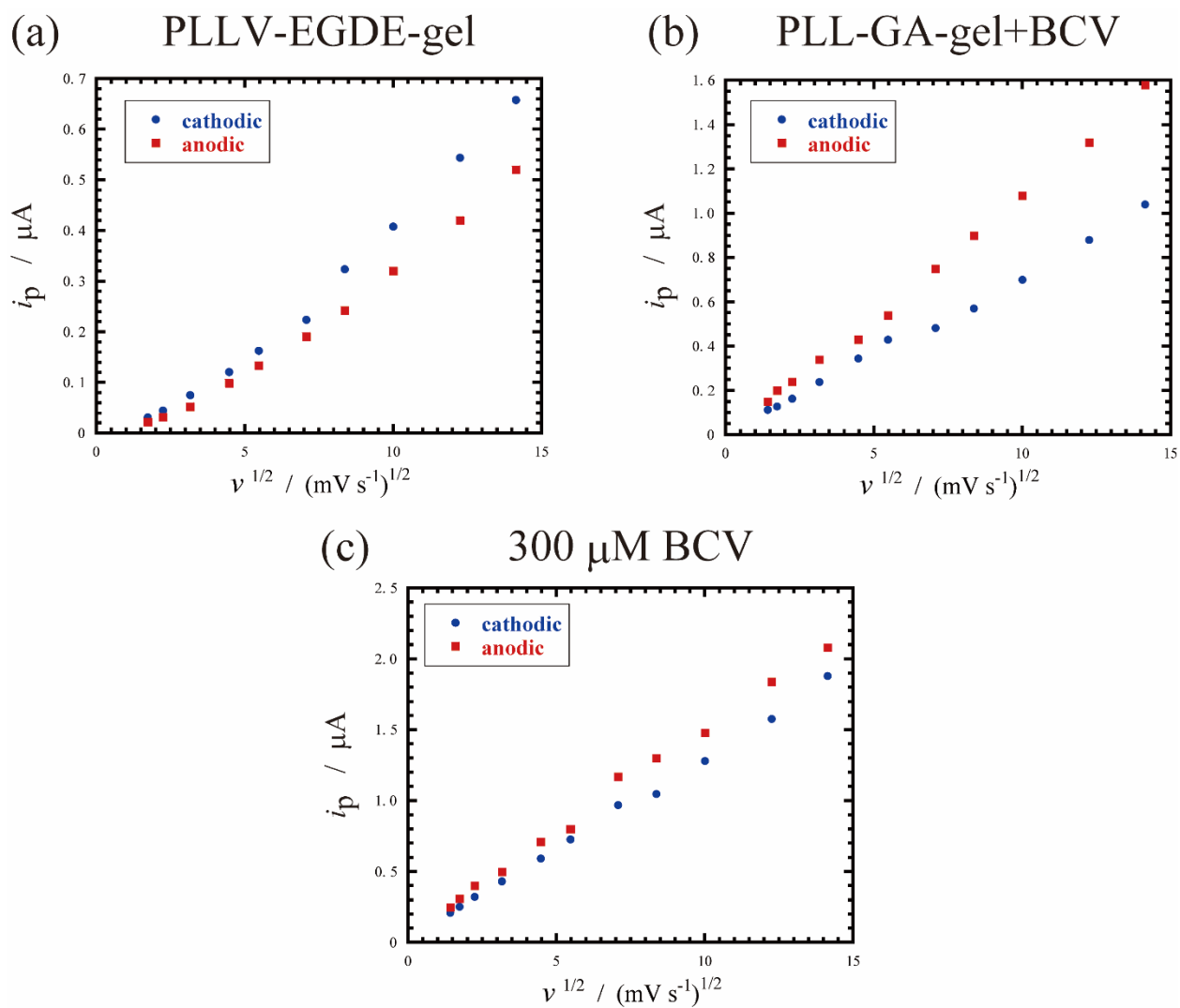


Fig. S3. Peak current vs. scan rate of (a) PLLV-EGDE-gel, (b) PLL-GA-gel + 200 μM BCV, and (c) 300 μM BCV. See Fig. 5 for details.

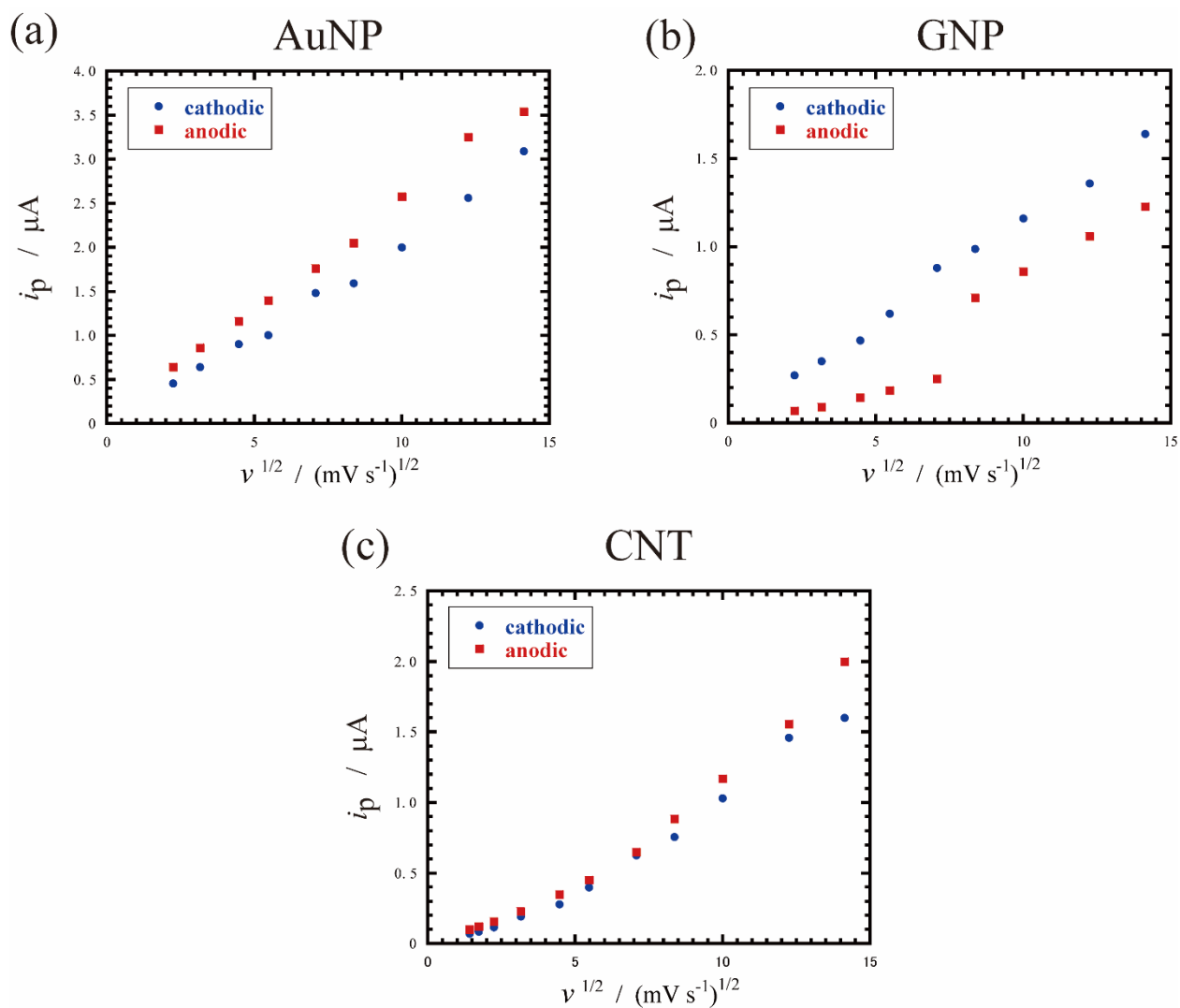


Fig. S4. Peak current vs. scan rate depend on incorporation of conductive fillers, (a) AuNP, (b) GNP, (c) CNT. See Fig. 8 for details.

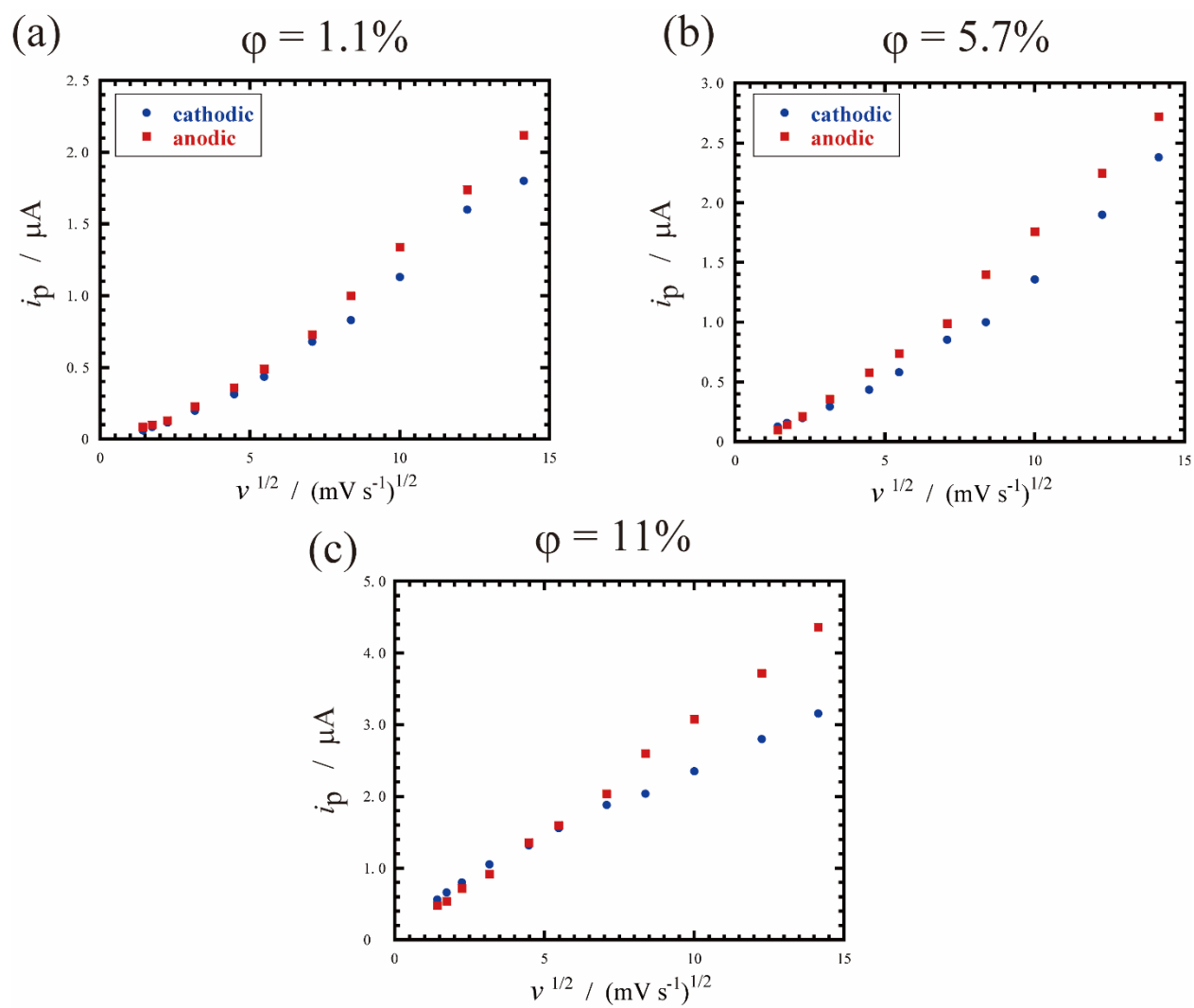


Fig. S5. Peak current vs. scan rate depend on incorporation of PSS, $\phi = 1.1\%$ (a), 5.7% (b), 11% (c). See Fig. 9 for details.

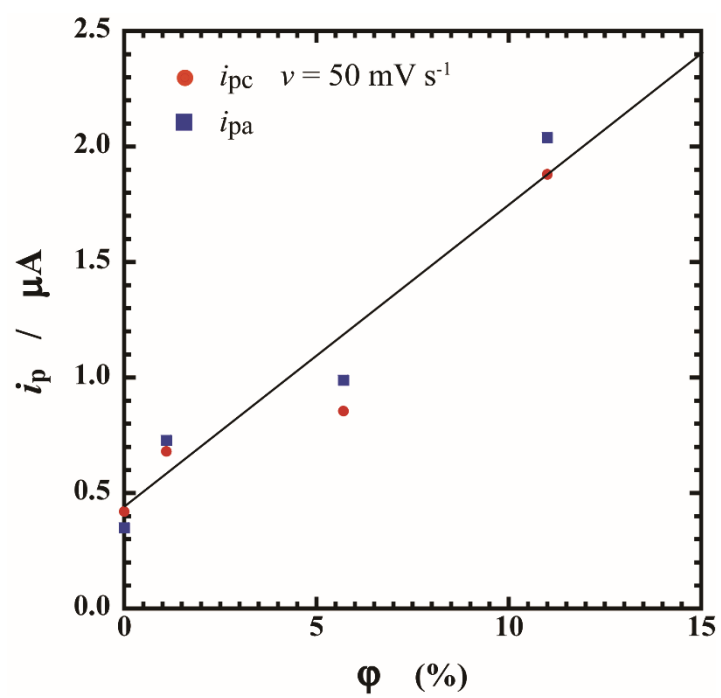


Fig. S6. Plot of i_p as a function of PSS content ϕ at $\nu = 50 \text{ mV s}^{-1}$.

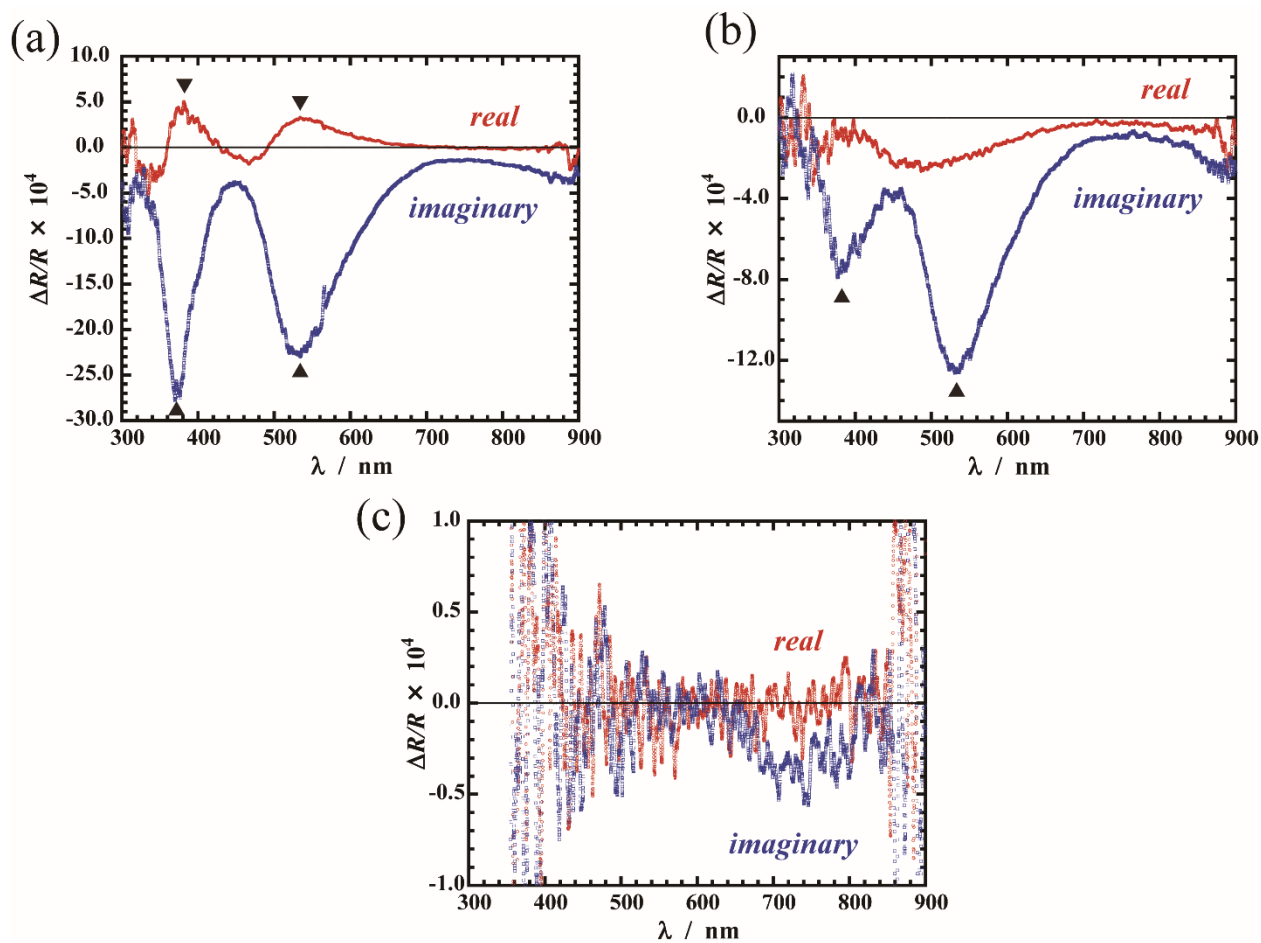


Fig. S7. ERS of the same PLLV-GA-gel with PSS used for CV measurements in PB solution. Potential modulation, $70 \text{ mV}_{\text{rms}}$ at a frequency of 14 Hz with $E_{\text{dc}} = E_{\text{m}}$. (a) $\phi = 1.1\%$, (b) $\phi = 5.7\%$, (c) $\phi = 11\%$. $V^{\bullet+}$ dimer bands, 371 nm, 533 nm, and ~ 860 nm, are marked by solid triangles.